Hindawi
Advances in Mathematical Physics
Volume 2021, Article ID 3445894, 22 pages
https://doi.org/10.1155/2021/3445894

Research Article

Various Soliton Solutions and Asymptotic State Analysis for the Discrete Modified Korteweg-de Vries Equation

Zhe Lin, Xiao-Yong Wen, and Meng-Li Qin

School of Applied Science, Beijing Information Science and Technology University, Beijing 100192, China

Correspondence should be addressed to Xiao-Yong Wen; xiaoyongwen@bistu.edu.cn

Received 6 July 2021; Revised 2 September 2021; Accepted 20 September 2021; Published 6 October 2021

Academic Editor: Mohammad Mirzazadeh

Under investigation is the discrete modified Korteweg-de Vries (mKdV) equation, which is an integrable discretization of the continuous mKdV equation that can describe some physical phenomena such as dynamics of anharmonic lattices, solitary waves in dusty plasmas, and fluctuations in nonlinear optics. Through constructing the discrete generalized $(m, N-m)$-fold Darboux transformation for this discrete system, the various discrete soliton solutions such as the usual soliton, rational soliton, and their mixed soliton solutions are derived. The elastic interaction phenomena and physical characteristics are discussed and illustrated graphically. The limit states of diverse soliton solutions are analyzed via the asymptotic analysis technique. Numerical simulations are used to display the dynamical behaviors of some soliton solutions. The results given in this paper might be helpful for better understanding the physical phenomena in plasma and nonlinear optics.

1. Introduction

Nonlinear partial differential equations (NPDEs) such as Burgers equation, KdV equation, mKdV equation, and nonlinear Schrödinger (NLS) equation can describe many important physical phenomena in nonlinear optics, acoustic in the nonharmonized lattice, deep water waves, plasma environments, and so on (see [1–5] and the references therein). The explicit exact solutions, especially soliton solutions, of the NPDEs play a vital role in many practical applications [6]. The soliton structures are formed when an exact balance between nonlinearity and dispersion effects in NPDEs takes place, and the KdV-type equation can usually describe the evolution of the unmodulated soliton in the small amplitude [6]. Another type of envelope soliton (dark or bright soliton and rogue wave) is formed when wave group dispersion is in complete balance with the nonlinearity of the medium, and this type of envelope soliton is a localized modulated wave packet whose dynamics are governed by the family of the NLS equation [6]. The Gardner equation is also called combined KdV-mKdV equation which is widely applied in various branches of physics [7]. As is well known, the KdV equation possesses bright soliton structures; while the mKdV equation can admit bright solitons and shock wave solution, compared with the KdV and mKdV equations, the Gardner equation admits solitons of the hyperbolic functions and kink solutions [7]. The soliton collision is an interesting and important nonlinear phenomenon in the nonlinear medium, nonlinear dynamics of soliton collisions, and soliton phase shifts in the KdV, and mKdV equations are taken for discussion [6, 8, 9]. However, to the authors' knowledge, for the continuous KdV-type equation, this soliton collision phenomenon and phase shift analysis have been discussed more, but for the discrete KdV-type equation, the relevant research for soliton collision and phase shift is poor, so it is a meaningful research topic to extend this collision phenomenon to discrete nonlinear lattice equations.

Recently, discrete integrable nonlinear lattice equations, as spatially discrete analogues of NPDEs, have drawn widespread attention due to their appearance in a variety of fields such as the propagation of optical pulses in nonlinear optics, Langmuir wave in plasma physics, nonlinear lattice dynamics, population dynamics, anharmonic lattice dynamics, Bose-Einstein condensates, and propagation of electrical signals in circuits [10–14]. Searching for explicit exact

solutions, especially soliton solutions, is used for depicting and explaining such nonlinear phenomena described by the discrete nonlinear lattice models. Methods of constructing the soliton solutions of the discrete integrable models have been proposed and developed such as the discrete inverse scattering method [13], the discrete Hirota bilinear formalism method [14, 15], and the discrete Darboux transformation (DT) method [16–25]. Among them, the discrete DT based on corresponding Lax representation is a useful technique to solve the discrete nonlinear models and its main idea is to keep the corresponding Lax pair of these discrete equations unchanged. Recently, a discrete generalized $(m, N-m)$-fold DT method has been proposed by one of the present authors of this paper [24, 25]. Compared with the common discrete DT which can only give the usual soliton (US) solutions, the discrete generalized $(m, N-m)$-fold DT [24, 25] is a generalization of the common discrete DT and the main advantage of this method is that it can give not only the US solution but also the rational solutions (e.g., rouge wave solutions and rational soliton (RS) solutions) and mixed interaction solutions of US and rational solution [24, 25]. For the US solutions of discrete nonlinear models, there have been a lot of literature studies [16–23] but the study of rational solutions and mixed interaction solutions of US and rational solutions is still not sufficient and systematic. As far as we know, the asymptotic behaviors of RS solutions and mixed interaction soliton solutions of US and RS by using asymptotic analysis have not been studied yet.

Therefore, in this paper, via the discrete generalized $(m, N-m)$-fold DT and asymptotic analysis techniques, we are going to focus on the following discrete mKdV equation [26]:

$$\begin{aligned} q_{n,t} = {} & \left(1+q_n^2\right)\left[q_{n+2} - 2q_{n+1} + 2q_{n-1} - q_{n-2}\right. \\ & \left. + q_{n+1}^2\left(q_{n+2}+q_n\right) - q_{n-1}^2\left(q_n+q_{n-2}\right)\right], \end{aligned} \tag{1}$$

where $q_n = q(n,t)$ stand for the real function of the discrete variable n and time variable t, and $q_{n,t} = dq_n/dt$. Equation (1), which possesses more nonlinear terms, is different from the discrete mKdV equation in [13, 23, 27–30]. Moreover in [26], Suris has given an Ablowitz-Ladik hierarchy including equation (1), whose Lax pair admits

$$\begin{aligned} E\varphi_n &= L_n\varphi_n, L_n = \begin{pmatrix} \lambda & q_n \\ -q_n & \dfrac{1}{\lambda} \end{pmatrix}, \\ \varphi_{n,t} &= M_n\varphi_n, M_n = \begin{pmatrix} M_{11} & M_{12} \\ M_{21} & M_{22} \end{pmatrix}, \end{aligned} \tag{2}$$

with

$$\begin{aligned} M_{11} = {} & \lambda^4 + \left(q_nq_{n-1} - 2\right)\lambda^2 + \left(q_n^2 + q_{n-2}q_n\right)q_{n-1}^2 \\ & + \left(q_n^2q_{n+1} - 2q_n + q_{n+1}\right)q_{n-1} + q_{n-2}q_n - \frac{q_{n-1}q_n}{\lambda^2}, \\ M_{12} = {} & q_n\lambda^3 + \left(q_{n+1} + q_n^2q_{n-1} + q_n^2q_{n+1} - 2q_n\right)\lambda \\ & + \frac{q_{n-2} + q_nq_{n-1}^2 + q_{n-2}q_{n-1}^2 - 2q_{n-1}}{\lambda} + \frac{q_{n-1}}{\lambda^3}, \\ M_{21} = {} & -q_{n-1}\lambda^3 + \left(-q_{n-2} - q_nq_{n-1}^2 - q_{n-2}q_{n-1}^2 + 2q_{n-1}\right)\lambda \\ & + \frac{-q_{n+1} - q_n^2q_{n-1} - q_n^2q_{n+1} + 2q_n}{\lambda} - \frac{q_n}{\lambda^3}, \\ M_{22} = {} & -q_nq_{n-1}\lambda^2 + \left(q_n^2 + q_nq_{n-2}\right)q_{n-1}^2 + \left(q_n^2q_{n+1} - 2q_n + q_{n+1}\right)q_{n-1} \\ & + q_nq_{n-2} + \frac{q_{n-1}q_n - 2}{\lambda^2} + \frac{1}{\lambda^4}, \end{aligned} \tag{3}$$

where $\varphi_n = (\phi_n, \psi_n)^T$ is a basic solution of equation (2) (the superscript T means the vector transpose), λ is the spectral parameter, and the shift symbol E is defined by $Ef_n = f_{n+1}$. It is easy to find that the zero curvature equation

$$L_{n,t} = (EM_n)L_n - L_nM_n \tag{4}$$

can be calculated by compatible condition $\varphi_{n,t} = \varphi_{t,n}$, which is subject to equation (1). If we assume that $q_n = \varepsilon q(n\varepsilon)$ in equation (1) and to rescale time $t \mapsto t/2\varepsilon^2$, then, to send $\varepsilon \longrightarrow 0$, thus, equation (1) can be reduced to the following continuous mKdV equation [26, 31, 32]:

$$q_t = q_{xxx} \mp 6q_xq^2. \tag{5}$$

The above process is called the continuous limit from equation (5) to equation (1). The mKdV equation (5) is a model to describe acoustic in the nonharmonized lattice and also can be used to study solitary waves in dusty plasmas and fluctuations in nonlinear optics etc. [3–5, 33–39], so it is important to study equation (5) in the physical background and practical significance. In [13, 40, 41], the authors point out that the discrete models can preserve some properties of its corresponding continuous equations, so equation (1), taken as the corresponding discrete equation of equation (5), may also have potential applications in describing some physical phenomena such as dust solitary waves in dust plasma and fluctuations in nonlinear optics, which suggests that the study of equation (1) also might have important theoretical significance and practical application value. Based on what we know, the US solutions, RS solutions, their mixed interaction soliton solutions via the discrete generalized $(m, N-m)$-fold DT, and associated soliton limit states via the asymptotic analysis technique for equation (1) have not been investigated before.

Therefore, in this paper, we will further investigate equation (1) via the discrete generalized $(m, N-m)$-fold DT and we will study the asymptotic behaviors at infinity of diverse soliton solutions via the asymptotic analysis technique, via the discrete generalized $(m, N-m)$-fold DT. The rest of this paper is organized as follows. In Section 2, based on the known Lax representation (2), the discrete generalized $(m, N-m)$-fold DT of equation (1) will be constructed and

formulated. In Section 3, the different special cases of the discrete generalized $(m, N-m)$-fold DT method are used to derive various soliton solutions such as US solutions, RS solutions, and their mixed interaction soliton solutions and we will analyze the limit states of such obtained soliton solutions via asymptotic analysis. Meanwhile, we also will use numerical simulations to watch the solutions' dynamical behaviors so that we can comprehend or even predict the physical properties of solutions more clearly. Some conclusions are given in the final section.

2. Discrete Generalized $(m, N-m)$-Fold DT

In this section, we will build up the discrete generalized $(m, N-m)$-fold DT of equation (1). With Lax pair (2), we consider a gauge transformation in the following form:

$$\tilde{\varphi}_n = T_n(\lambda)\varphi_n, \tag{6}$$

which requires that $\tilde{\varphi}_n = (\tilde{\phi}_n, \tilde{\psi}_n)^T$ must be subject to $\tilde{\varphi}_n = \tilde{L}_n\tilde{\varphi}_n, \tilde{\varphi}_{n,t} = \tilde{M}_n\tilde{\varphi}_n$ according to the knowledge of DT, where $\tilde{L}_n, \tilde{M}_n$ have the same forms as L_n, M_n except by replacing its q_n with $\tilde{q}_n$. Moreover, $\tilde{L}_n, \tilde{M}_n$ and L_n, M_n also admit the following identities:

$$\tilde{L}_n = T_{n+1}L_nT_n^{-1}, \tilde{M}_n = (T_{n,t} + T_nM_n)T_n^{-1}. \tag{7}$$

To this aim, we construct a special N-order Darboux matrix T_n defined by

$$T_n(\lambda) = \begin{pmatrix} \lambda^{2N} + \sum_{j=0}^{N-1} a_n^{(2j)}\lambda^{2j} & \sum_{j=0}^{N-1} b_n^{(2j+1)}\lambda^{2j+1} \\ -\sum_{j=0}^{N-1} b_n^{(2j+1)}\lambda^{2N-2j-1} & 1 + \sum_{j=0}^{N-1} a_n^{(2j)}\lambda^{2N-2j} \end{pmatrix}, \tag{8}$$

in which N is a positive integer and $a_n^{(2j)}$ and $b_n^{(2j+1)}$ are some unknown functions of n, t and can be determined by

$$\begin{gathered} T_n^{(0)}(\lambda_i)\varphi_n^{(0)}(\lambda_i) = 0, \\ T_n^{(0)}(\lambda_i)\varphi_n^{(1)}(\lambda_i) + T_n^{(1)}(\lambda_i)\varphi_n^{(0)}(\lambda_i) = 0, \\ \cdots\cdots, \\ \sum_{j=0}^{m_i} T_n^{(j)}(\lambda_i)\varphi_n^{(m_i-j)}(\lambda_i) = 0, \end{gathered} \tag{9}$$

where $N = n + \sum_{j=0}^{n} m_i\,(i = 1, 2, \cdots, n)$ and $T_n^{(j)}$ is given by $T_n(\lambda_i + \varepsilon) = \sum_{k=0}^{N} T_n^{(k)}(\lambda_i)\varepsilon^k$, while $\varphi_n^{(j)}$ is derived by $\varphi_n(\lambda_i + \varepsilon) = \varphi_n^{(0)}(\lambda_i) + \varphi_n^{(1)}(\lambda_i)\varepsilon + \varphi_n^{(2)}(\lambda_i)\varepsilon^2 + \cdots$, in which $\varphi_n^{(k)}(\lambda_i) = (1/k!)(\partial^k/\partial\lambda^k)\varphi_n(\lambda)|_{\lambda=\lambda_i} = ((1/k!)(\partial^k/\partial\lambda^k)\phi_n(\lambda)|_{\lambda=\lambda_i}, (1/k!)(\partial^k/\partial\lambda^k)\psi_n(\lambda)|_{\lambda=\lambda_i})^T$. By explaining the above research processes and conditions, we conclude the following generalized $(m, N-m)$-fold DT theorem of equation (1):

Theorem 1. *Let $\varphi_n(\lambda_i) = (\phi_n(\lambda_i), \psi_n(\lambda_i))^T$ be m column vector solutions of Lax pair (2) with the special parameter λ_i $(i = 1, 2, \cdots, m)$ and the initial seed solution q_0 of equation (1), and then, the generalized $(m, N-m)$-fold DT from the old solution q_n to the new one $\tilde{q}_n$ is given by*

$$\tilde{q}_n = q_n a_{n+1}^{(0)} + b_{n+1}^{(1)}, \tag{10}$$

with

$$a_{n+1}^{(0)} = \frac{\Delta a_{n+1}^{(0)}}{\Delta_n}, b_n^{(1)} = \frac{\Delta b_{n+1}^{(1)}}{\Delta_n}, \Delta_N = \det\left(\left[\Delta_{m_1+1}^{(1)}, \Delta_{m_2+1}^{(2)}, \cdots, \Delta_{m_n+1}^{(m)}\right]^T\right), \tag{11}$$

where $\Delta_{m_i+1}^{(i)} = (\Delta_{j,s}^{(i)})_{2(m_i+1)\times 2N}$, in which $\Delta_{j,s}^{(i)}(1 \le j \le 2m_i + 2, 1 \le s \le 2N)$ be given by following formulae:

$$\Delta_{j,s}^{(i)} = \begin{cases} \sum_{k=0}^{j-1} C_{2N-2s}^k \lambda_i^{2N-2s-k}\phi_i^{(j-1-k)}, & \text{for } 1 \le j \le m_i + 1, 1 \le s \le N, \\ \sum_{k=0}^{j-1} C_{4N-2s+1}^k \lambda_i^{4N-2s-k+1}\psi_i^{(j-1-k),} & \text{for } 1 \le j \le m_i + 1, N+1 \le s \le 2N, \\ \sum_{k=0}^{j-(N+1)} C_{2s}^k \lambda_i^{(2s-k)}\psi_i^{(j-1-N-k),} & \text{for } m_i + 2 \le j \le 2(m_i+1), 1 \le s \le N, \\ -\sum_{k=0}^{j-(N+1)} C_{2s-2N-1}^k \lambda_i^{(2s-2N-k-1)}\phi_i^{(j-N-1-k)}, & \text{for } m_i + 2 \le j \le 2(m_i+1), N+1 \le s \le 2N, \end{cases} \tag{12}$$

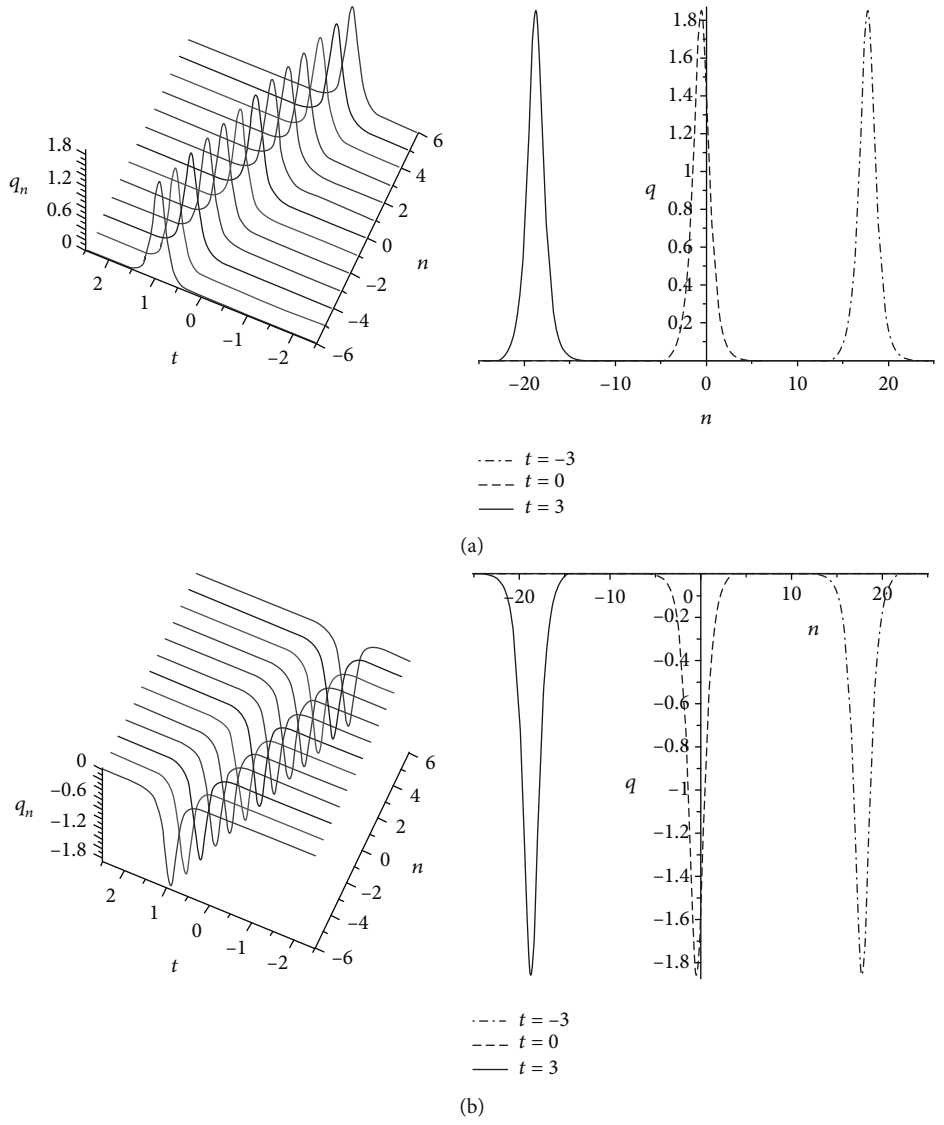

Figure 1: One-soliton solution $\tilde{q}_n$ in (15) or (17). (a1) Bell-shaped one-soliton solution with the parameter $\lambda_1 = 1/2$. (b1) Anti-bell-shaped one-soliton solution with the parameter $\lambda_1 = 2$. (a2, b2) The propagation processes for $\tilde{q}_n$ at $t = -3$ (dash-dot line), $t = 0$ (long dashed line), and $t = 3$ (solid line).

and $\Delta B^{(N-1)}$ *are given by the determinant* Δ_N^{ε} *replacing its* $(N+1)$*th columns by the column vector* $(g^{(1)},\cdots,g^{(n)})^T$ *with* $g^{(i)} = (g_j^i)_{2(m_i+1)\times 1}$ *in which*

$$g_j^i = \begin{cases} -\sum_{k=0}^{j-1} C_{2N}^k \lambda_i^{2N-k} \phi_i^{(j-1-k)}, & \text{for } 1 \le j \le m_i + 1, \\ -\sum_{k=0}^{j-N-1} C_{2N}^k \lambda_i^{(2N-k)} \psi_i^{(j-N-1-k)}, & \text{for } m_i + 2 \le j \le 2(m_i+1). \end{cases} \tag{13}$$

Remark 2. It is worth pointing out that m in the notation "$(m, N-m)$-fold" means that the number of the distinct spectral parameters and $N-m$ means the sum of the orders of the Taylor series of the vector eigenfunction φ_n. If $n = N$ and $m_i = 0\,(1 \le i \le N)$, the generalized $(m, N-m)$-fold DT is converted to the $(N, 0)$-fold DT which includes the usual N-fold DT, from which we can develop the usual N-soliton solutions starting from zero seed or nonzero constant seed solution of equation (1). If $m = 1$, the above generalized $(m, N-m)$-fold DT reduces to the generalized $(1, N-1)$-fold one, from which we can derive higher-order RS solutions of equation (1). If $m = 2$, the above generalized $(m, N-m)$-fold DT reduces to the generalized $(2, N-2)$-fold one, from which we can derive mixed soliton solutions of the US and RS to equation (1). It is not hard to find that the N-fold DT, generalized $(1, N-1)$-fold DT, and generalized $(2, N-2)$-fold DT are three special cases of the generalized $(m, N-m)$-fold DT. Besides, if $2 < m < N$, one can use the generalized $(m, N-m)$-fold DT to give complex mixed interaction soliton solutions. For more details of Theorem 1, the reader can refer to [23–25] and the references therein, so we omit the detailed proof here.

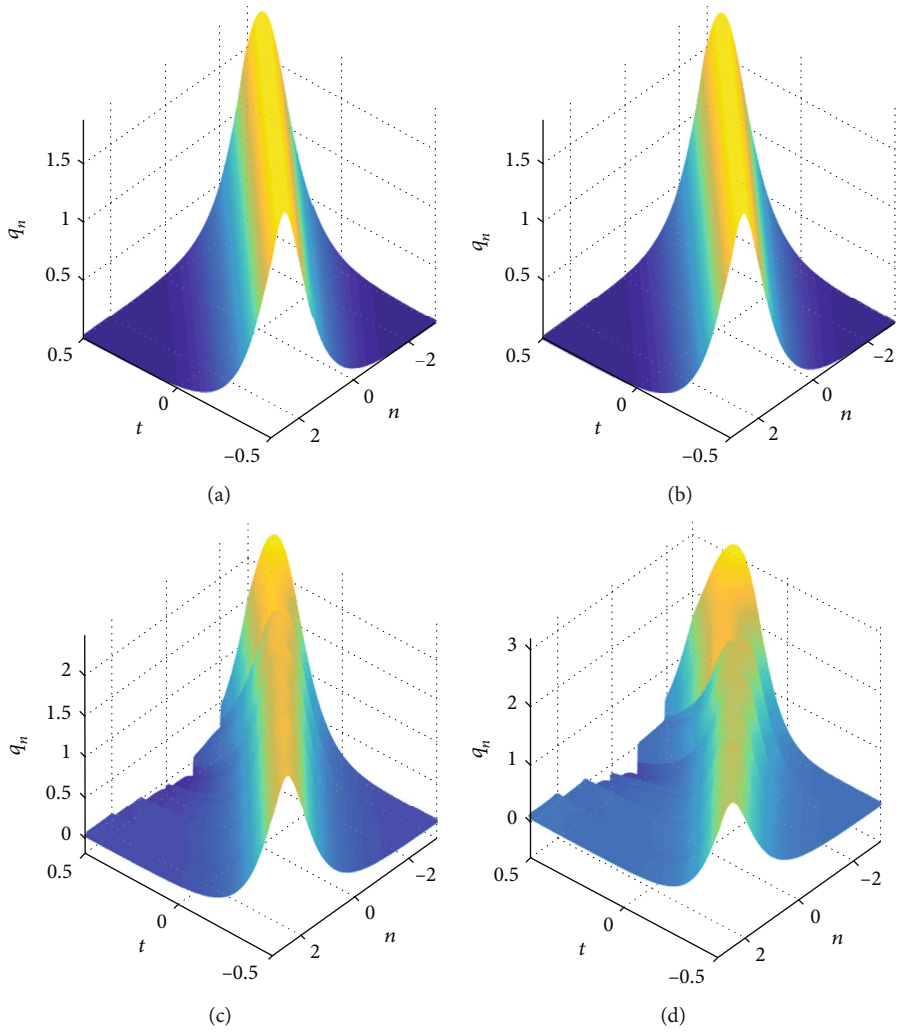

FIGURE 2: One-soliton solution (17) with the same parameter as in Figure 1. (a) Exact solution. (b) Time evolution without a small noise. (c) Time evolution with a 2% noise. (d) Time evolution with a 5% noise.

3. Applications of the Generalized $(m, N-m)$-Fold DT

In the previous section, we have constructed the discrete generalized $(m, N-m)$-fold DT of equation (1). So, in this section, we will use the generalized $(m, N-m)$-fold DT to get various soliton solutions, like US solutions, RS solutions, and their mixed soliton solutions and then analyze the elastic interaction and limit state of such solitons by using asymptotic analysis.

3.1. Usual N-Soliton Solutions and Their Asymptotic Analysis. We can get usual soliton solutions from the vanishing background by using N-fold DT, namely, in the condition of $m = N$ in discrete generalized $(m, N-m)$-fold DT. Substituting the initial solutions $q_n = 0$ into Lax pair (2) can give its basic solution:

$$\varphi_n = \begin{pmatrix} \phi_n \\ \psi_n \end{pmatrix} = \begin{pmatrix} \lambda^n e^{\left(\lambda^4 - 2\lambda^2\right)t} \\ \lambda^{-n} e^{\left(\frac{1}{\lambda^4} - \frac{2}{\lambda^2}\right)t} \end{pmatrix}. \tag{14}$$

From equation (10), we can derive the exact soliton solutions of equation (1). In order to comprehend them more intuitively, the evolution structures of soliton solutions are shown in Figures 1–4 when N=1,2,3.

(I) when N=1, let $\lambda = \lambda_1$; based on the N-fold DT, we can get the onefold exact solution as

$$\tilde{q}_n = b_{n+1}^{(1)}, \tag{15}$$

where $b_n^{(1)} = \Delta b_n^{(1)} / \Delta_n$, in which

$$\begin{aligned} \Delta_n &= \begin{vmatrix} \phi_n(\lambda_1) & \lambda_1 \psi_n(\lambda_1) \\ \lambda_1^2 \psi_n(\lambda_1) & -\lambda_1 \phi_n(\lambda_1) \end{vmatrix}, \\ \Delta b_n^{(1)} &= \begin{vmatrix} \phi_n(\lambda_1) & -\lambda_1^2 \phi_n(\lambda_1) \\ \lambda_1^2 \psi_n(\lambda_1) & -\psi_n(\lambda_1) \end{vmatrix}, \end{aligned} \tag{16}$$

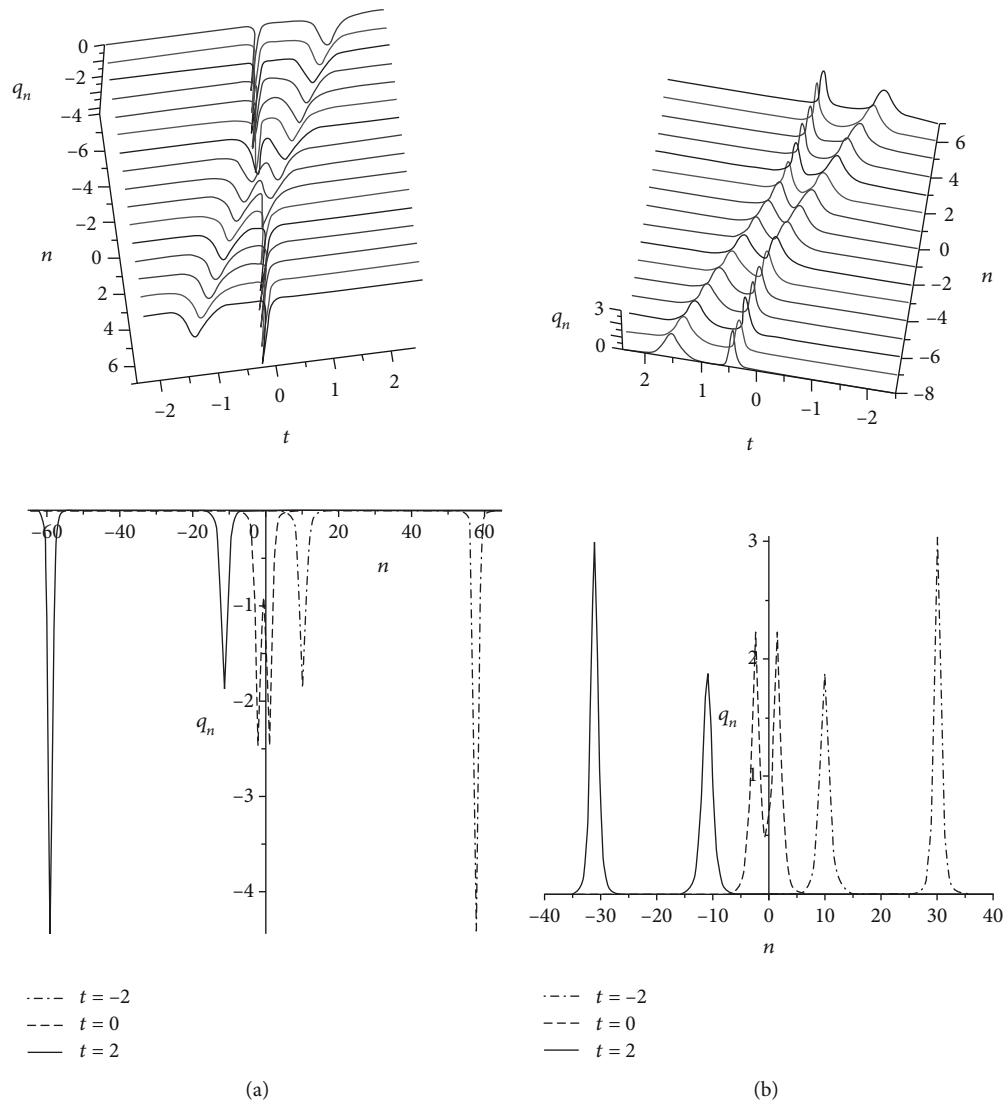

(a) (b)

Figure 3: Continued.

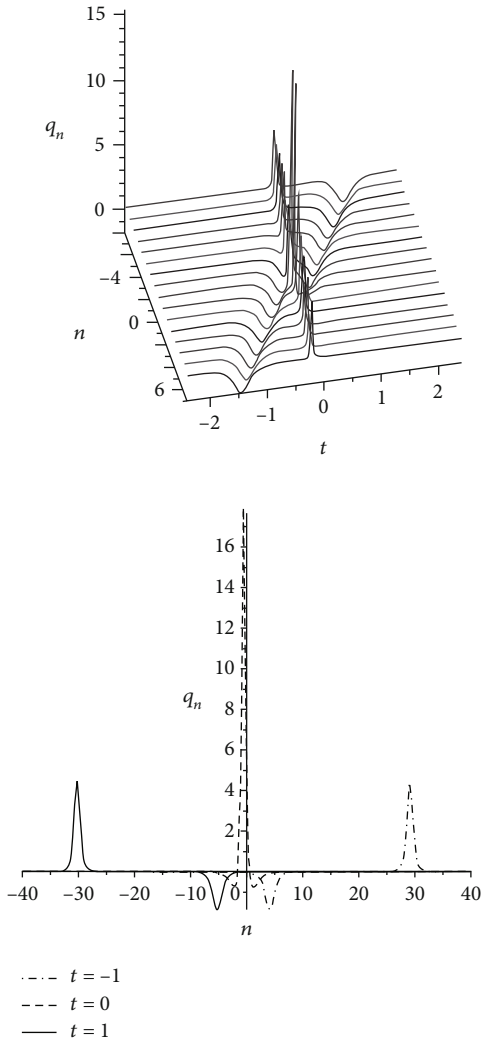

(c)

FIGURE 3: Two-soliton solution $\tilde{q}_n$ in (18) or (20). (a1) Two anti-bell-shaped solitons with parameters $\lambda_1 = 2, \lambda_2 = 1/3$. (b1) Two bell-shaped solitons with parameters $\lambda_1 = 5/2, \lambda_2 = 1/2$. (c1) Bell-shaped soliton and anti-bell-shaped soliton with parameters $\lambda_1 = 2$ and $\lambda_2 = 3$. (a2–c2) The propagation processes for $\tilde{q}_n$ at different time corresponding to (a1–c1), respectively.

while $b_{n+1}^{(1)}$ is obtained from $b_n^{(1)}$ by replacing n with $n+1$.

After bringing (14) into equation (15), we will get the usual one-soliton solution. In order to explore its physical characteristics, this solution can be rewritten as

$$\tilde{q}_n = \frac{1-\lambda_1^4}{2\lambda_1^2}\ \text{sech}\ (\xi_1 + \ln\lambda_1), \tag{17}$$

where $\xi_1 = (2\ln\lambda_1)n + (\lambda_1^4 - (1/\lambda_1^4) + (2/\lambda_1^2) - 2\lambda_1^2)t$ and $\lambda_1 > 0$ is a spectrum parameter. In this special one-solution form, we can easily explore its important physical quantities such as amplitude, width, velocity, wave number, primary phase, and energy, which are listed in Table 1. Here, the energy of q_n is defined by $E_{q_n} = \int_{-\infty}^{\infty} q_n^2 dn$.

From the above analysis, we can find that q_n is the bell-shaped bright one-soliton when $0 < \lambda_1 < 1$ and anti-bell-shaped one-soliton when $\lambda_1 > 1$. When $\lambda_1 = 1/2$ and $\lambda_1 = 2$, Figure 1 presents the evolution structures of bell-shaped one-soliton and anti-bell-shaped one-soliton, respectively.

Next, adopting the finite difference method [42], we can simulate the soliton solutions numerically, which can show the dynamical behaviors and propagation stability of one-soliton solutions more clearly. Figure 2 shows the exact one-soliton solution (17) of equation (1), time evolutions using exact one-soliton solution (17), and the results of adding 2% and 5% perturbations to the exact one-soliton solution. As can be seen, Figures 2(a) and 2(b) show that the representation of time evolutions for solution (17) without noise almost keeps in line with the exact solution (17) in time $t \in (-0.5, 0.5)$, which shows the accuracy of our numerical simulation. Compared with the unperturbed solution, Figures 2(c) and 2(d) exhibit that if we add 2% and 5% perturbations to the initial exact solution, the wave propagation performs a relatively small oscillation in time $t \in (-0.5, 0.5)$, that is to say that the numerical results in Figure 2 show that

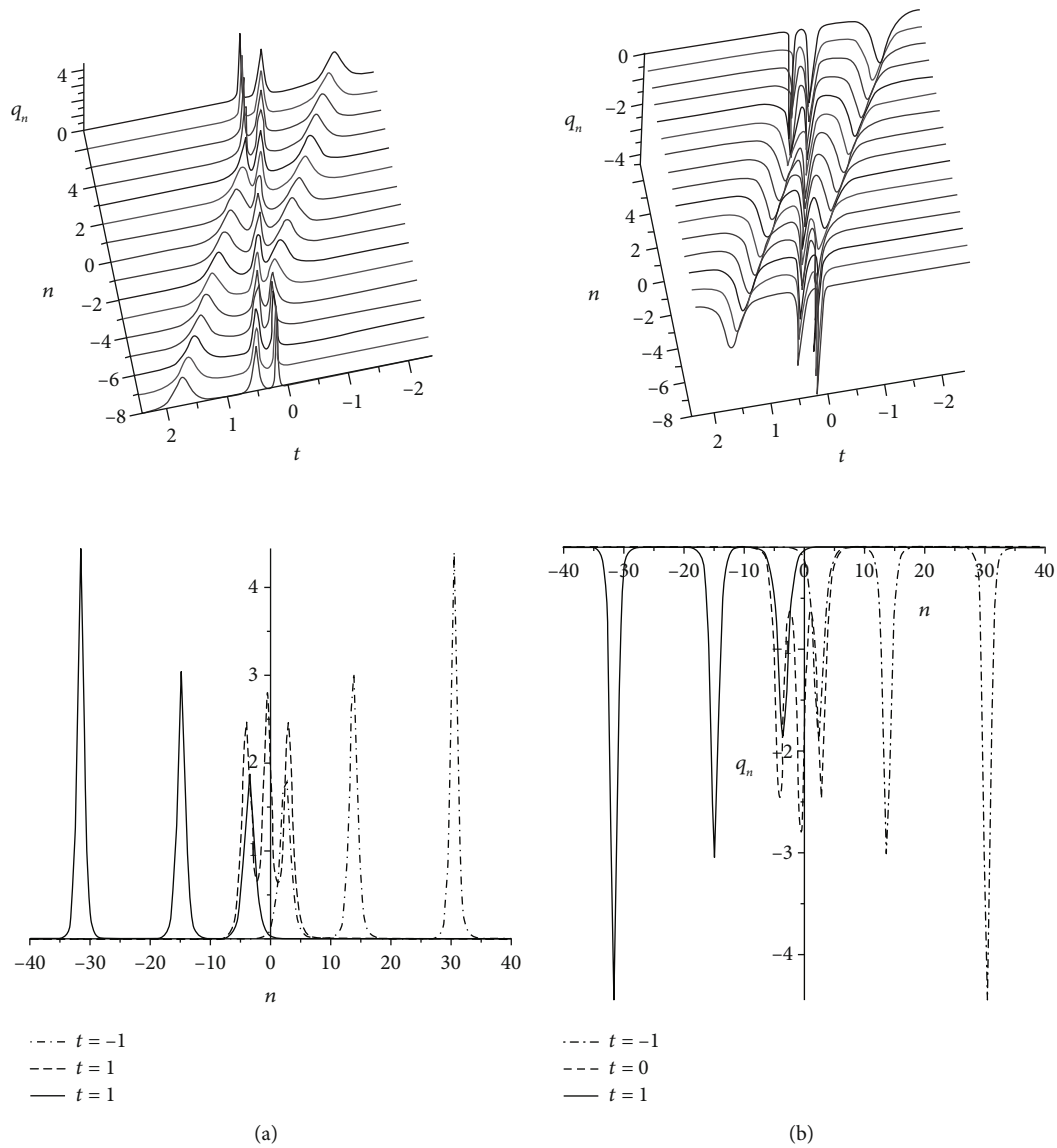

Figure 4: Continued.

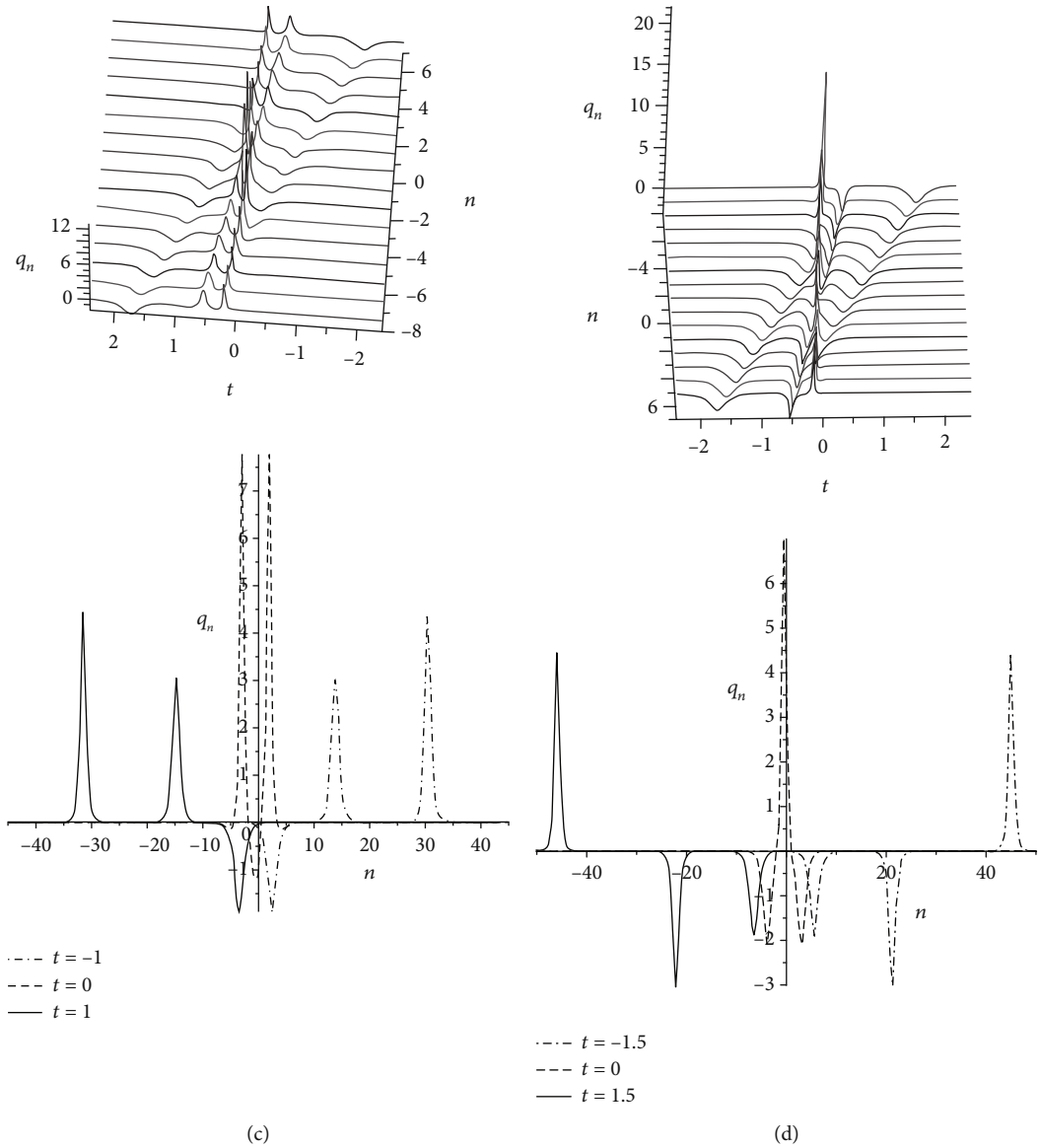

Figure 4: Three-soliton solution $\tilde{q}_n$ in (23). (a1) Bell-shaped three solitons with parameters $\lambda_1 = 5/2, \lambda_2 = 1/2, \lambda_2 = 1/3$. (b1) Anti-bell-shaped three solitons with parameters $\lambda_1 = 2, \lambda_2 = 2/5, \lambda_2 = 3$. (c1) Two bell-shaped solitons and one anti-bell-shaped soliton with parameters $\lambda_1 = 5/2, \lambda_2 = 2, \lambda_2 = 1/3$. (d1) Two anti-bell-shaped solitons and one bell-shaped soliton with parameters $\lambda_1 = 2, \lambda_2 = 2/5, \lambda_2 = 1/3$. (a2–d2) The propagation processes for $\tilde{q}_n$ at different time corresponding to (a1–d1), respectively.

Table 1: Physical characteristics of the one-soliton solution.

Soliton	Amplitude	Width	Velocity	Wave number	Primary phase	Energy
q_n	$\left(1-\lambda_1^4\right)/2\lambda_1^2$	$(1/2\ln\lambda_1)$	$\left(\lambda_1^8-2\lambda_1^6+2\lambda_1^2-1\right)/2\lambda_1^4\ln\lambda_1$	$2\ln\lambda_1$	$\ln\lambda_1$	$\left(\lambda_1^4-1\right)^2/4\lambda_1^4\lvert\ln\lambda_1\rvert$

Table 2: Physical characteristics of the two-soliton solution.

Solitons	Amplitudes	Widths	Velocities	Wave number	Primary phases	Energies
q_1^-	$\left(\lambda_1^4-1\right)/2\lambda_1^2$	$1/2\ln\lambda_1$	$\left(\lambda_1^8-2\lambda_1^6+2\lambda_1^2-1\right)/2\lambda_1^4\ln\lambda_1$	$2\ln\lambda_1$	$\ln\left\lvert\left(\lambda_1\left(\lambda_1^2-\lambda_2^2\right)\right)/\left(\lambda_1^2\lambda_2^2-1\right)\right\rvert$	$\left(\lambda_1^4-1\right)^2/4\lambda_1^4\lvert\ln\lambda_1\rvert$
q_2^-	$\left(1-\lambda_2^4\right)/2\lambda_2^2$	$1/2\ln\lambda_2$	$\left(\lambda_2^8-2\lambda_2^6+2\lambda_2^2-1\right)/2\lambda_2^4\ln\lambda_2$	$2\ln\lambda_2$	$\ln\left\lvert\left(\lambda_2\left(\lambda_1^2\lambda_2^2-1\right)\right)/\left(\lambda_1^2-\lambda_2^2\right)\right\rvert$	$\left(\lambda_2^4-1\right)^2/4\lambda_2^4\lvert\ln\lambda_2\rvert$
q_1^+	$\left(\lambda_1^4-1\right)/2\lambda_1^2$	$1/2\ln\lambda_1$	$\left(\lambda_1^8-2\lambda_1^6+2\lambda_1^2-1\right)/2\lambda_1^4\ln\lambda_1$	$2\ln\lambda_1$	$\ln\left\lvert\left(\lambda_2\left(\lambda_1^2\lambda_2^2-1\right)\right)/\left(\lambda_1^2-\lambda_2^2\right)\right\rvert$	$\left(\lambda_1^4-1\right)^2/4\lambda_1^4\lvert\ln\lambda_1\rvert$
q_2^+	$\left(1-\lambda_2^4\right)/2\lambda_2^2$	$1/2\ln\lambda_2$	$\left(\lambda_2^8-2\lambda_2^6+2\lambda_2^2-1\right)/2\lambda_2^4\ln\lambda_2$	$2\ln\lambda_2$	$\ln\left\lvert\left(\lambda_1\left(\lambda_1^2-\lambda_2^2\right)\right)/\left(\lambda_1^2\lambda_2^2-1\right)\right\rvert$	$\left(\lambda_2^4-1\right)^2/4\lambda_2^4\lvert\ln\lambda_2\rvert$

Table 3: The relationship between parameters and shapes of two solitons.

Soliton	Parameters	Shapes
q_n	$\lambda_1 > 1, 0 < \lambda_2 < 1$ and $\lambda_1 > 1/\lambda_2$	BS-BS
	$0 < \lambda_1 < 1, \lambda_2 > 1$ and $\lambda_2 > 1/\lambda_1$	BS-BS
	$\lambda_1, \lambda_2 > 1$ or $0 < \lambda_1, \lambda_2 < 1$	BS-ABS
	$0 < \lambda_1 < 1, \lambda_2 > 1$ and $\lambda_2 < 1/\lambda_1$	ABS-ABS
	$\lambda_1 > 1, 0 < \lambda_2 < 1$ and $\lambda_1 < 1/\lambda_2$	ABS-ABS

BS stands for bell-shaped soliton, while ABS stands for anti-bell-shaped soliton.

the evolution of the exact one-soliton solution is robust against a small noise.

(II) when N=2, let $\lambda = \lambda_i\,(i = 1, 2)$; we can get the two-fold exact solution from the transformation (10) as

$$\tilde{q}_n = b_{n+1}^{(1)}, \tag{18}$$

where $b_n^{(1)} = \Delta b_n^{(1)}/\Delta_n$, in which

$$\Delta_n = \begin{vmatrix} \lambda_1^2\phi_n(\lambda_1) & \phi_n(\lambda_1) & \lambda_1^3\psi_n(\lambda_1) & \lambda_1\psi_n(\lambda_1) \\ \lambda_2^2\phi_n(\lambda_2) & \phi_n(\lambda_2) & \lambda_2^3\psi_n(\lambda_2) & \lambda_2\psi_n(\lambda_2) \\ \lambda_1^2\psi_n(\lambda_1) & \lambda_1^4\psi_n(\lambda_1) & -\lambda_1\phi_n(\lambda_1) & -\lambda_1^3\phi_n(\lambda_1) \\ \lambda_2^2\psi_n(\lambda_2) & \lambda_2^4\psi_n(\lambda_2) & -\lambda_2\phi_n(\lambda_2) & -\lambda_2^3\phi_n(\lambda_2) \end{vmatrix},$$

$$\Delta b_n^{(1)} = \begin{vmatrix} \lambda_1^2\phi_n(\lambda_1) & \phi_n(\lambda_1) & \lambda_1^3\psi_n(\lambda_1) & -\lambda_1^4\phi_n(\lambda_1) \\ \lambda_2^2\phi_n(\lambda_2) & \phi_n(\lambda_2) & \lambda_2^3\psi_n(\lambda_2) & -\lambda_2^4\phi_n(\lambda_2) \\ \lambda_1^2\psi_n(\lambda_1) & \lambda_1^4\psi_n(\lambda_1) & -\lambda_1\phi_n(\lambda_1) & -\psi_n(\lambda_1) \\ \lambda_2^2\psi_n(\lambda_2) & \lambda_2^4\psi_n(\lambda_2) & -\lambda_2\phi_n(\lambda_2) & -\psi_n(\lambda_2) \end{vmatrix}, \tag{19}$$

while $b_{n+1}^{(1)}$ is obtained from $b_n^{(1)}$ by replacing n with $n+1$. For the sake of analysis, solution (18) can be rewritten as

$$\tilde{q}_n = \frac{\left(\lambda_1^2\lambda_2^2 - 1\right)\left(\lambda_1^2 - \lambda_2^2\right)\left[\lambda_1^2\left(1 - \lambda_2^4\right)\cos h(\eta_1 + \ln\lambda_1) - \lambda_2^2\left(1 - \lambda_1^4\right)\cos h(\eta_2 + \ln\lambda_2)\right]}{\lambda_1^2\lambda_2^2\left[\left(\lambda_1^2 - \lambda_2^2\right)^2\cos h(\eta_1 + \ln\lambda_1 + \eta_2 + \ln\lambda_2) + \left(\lambda_1^2\lambda_2^2 - 1\right)^2\cos h(\eta_1 + \ln\lambda_1 - \eta_2 - \ln\lambda_2) - \left(1 - \lambda_1^4\right)\left(1 - \lambda_2^4\right)\right]}, \tag{20}$$

where $\eta_i = (2\ln\lambda_i)n + (\lambda_i^4 - (1/\lambda_i^4) + (2/\lambda_i^2) - 2\lambda_i^2)t$, $(i = 1, 2)$, in which $\lambda_i > 0$ is a spectrum parameter.

According to the ideas of [18, 43–45], we perform asymptotic analysis of solution (20), from which we can easily work out the limit state expressions of solution $\tilde{q}_n$ before and after the interaction. And the detailed physical quantities are listed in Table 2.

Before the interactions $(t \longrightarrow -\infty)$,

$$\begin{aligned} &\tilde{q}_n \longrightarrow q_1^- = \frac{\lambda_1^4 - 1}{2\lambda_1^2}\,\mathrm{sech}\left(\eta_1 + \ln\lambda_1 + \ln\left|\frac{\lambda_1^2 - \lambda_2^2}{\lambda_1^2\lambda_2^2 - 1}\right|\right), \quad (\eta_1 \sim 0, \eta_2 \longrightarrow +\infty), \\ &\tilde{q}_n \longrightarrow q_2^- = -\frac{\lambda_2^4 - 1}{2\lambda_2^2}\,\mathrm{sech}\left(\eta_2 + \ln\lambda_2 - \ln\left|\frac{\lambda_1^2 - \lambda_2^2}{\lambda_1^2\lambda_2^2 - 1}\right|\right), \quad (\eta_2 \sim 0, \eta_1 \longrightarrow +\infty), \end{aligned} \tag{21}$$

where q_1^-, q_2^- are the asymptotic state expressions of $\tilde{q}_n$ before the interaction.

After the interactions $(t \longrightarrow +\infty)$,

$$\begin{aligned} &\tilde{q}_n \longrightarrow q_1^+ = \frac{\lambda_1^4 - 1}{2\lambda_1^2}\,\mathrm{sech}\left(\eta_1 + \ln\lambda_1 - \ln\left|\frac{\lambda_1^2 - \lambda_2^2}{\lambda_1^2\lambda_2^2 - 1}\right|\right), \quad (\eta_1 \sim 0, \eta_2 \longrightarrow +\infty), \\ &\tilde{q}_n \longrightarrow q_2^+ = -\frac{\lambda_2^4 - 1}{2\lambda_2^2}\,\mathrm{sech}\left(\eta_2 + \ln\lambda_2 + \ln\left|\frac{\lambda_1^2 - \lambda_2^2}{\lambda_1^2\lambda_2^2 - 1}\right|\right), \quad (\eta_2 \sim 0, \eta_1 \longrightarrow +\infty), \end{aligned} \tag{22}$$

where q_1^+, q_2^+ are the asymptotic state expressions of $\tilde{q}_n$ after the interaction.

From the above analysis, we can see that the characteristics and embodiment of the two-soliton solution in the physical field can be summarized as follows: (i) the amplitude, velocities, and energy of q_n remain unchanged before and after the interactions; (ii) after the soliton interactions, the phase shifts of two solitons are $-2\ln|(\lambda_1^2 - \lambda_2^2)/(\lambda_1^2\lambda_2^2 - 1)|$ and $2\ln|(\lambda_1^2 - \lambda_2^2)/(\lambda_1^2\lambda_2^2 - 1)|$; and (iii) the soliton width, wave number, and wave shapes are related to two spectrum parameters $\lambda_i (i = 1, 2)$, and the relationship between shapes and parameters are shown in Table 3.

The corresponding evolution plots of solution (18) or (20) can be also elaborated clearly. When the parameters $\lambda_1 = 2$ and $\lambda_2 = 1/3$, we can see that the overtaking elastic interactions between two unidirectional anti-bell-shaped solitons on the vanishing background in Figures 3(a1) and 3(a2); when we choose the parameters $\lambda_1 = 5/2$ and $\lambda_2 = 1/2$, the overtaking elastic interactions between two unidirectional bell-shaped solitons on the vanishing background are shown in Figures 3(b1) and 3(b2); in Figures 3(c1) and 3(c2), we can also see the overtaking elastic interactions between unidirectional bell-shaped soliton and anti-bell-shaped soliton on the vanishing background when $\lambda_1 = 2$ and $\lambda_2 = 3$.

Comparing Figures 3(c1) and 3(c2) with Figures 3(a1)–3(b2), we find that the soliton amplitude in Figures 3(c1)

and 3(c2) is obviously higher than that in Figures 3(a1)–3(b2). In Figures 3(c1) and 3(c2), we can clearly see that the soliton interaction occurs at $t = 0$ and the high amplitude occurs near the origin; if we choose $n = t = 0$, then, from solution (20), we have $\tilde{q}_n = (1 - (1/\lambda_1\lambda_2))(\lambda_1 + \lambda_2)$. As $\lambda_1\lambda_2$ approaches 1, the value of $\tilde{q}_n$ is small. However, when both λ_1 and λ_2 are greater than 1, the value of $\tilde{q}_n$ is larger. Therefore, we can infer that the choice of parameters λ_1 and λ_2 determines the amplitude, shape, and energy of the soliton.

(III) when N=3, let $\lambda = \lambda_i\ (i = 1, 2, 3)$; we can get the threefold exact solution from the transformation (10):

$$\tilde{q}_n = b_{n+1}^{(1)}, \tag{23}$$

where $b_n^{(1)} = \Delta b_n^{(1)}/\Delta_n$, in which

$$\Delta_n = \begin{vmatrix} \lambda_1^4\phi_n(\lambda_1) & \lambda_1^2\phi_n(\lambda_1) & \phi_n(\lambda_1) & \lambda_1^5\psi_n(\lambda_1) & \lambda_1^3\psi_n(\lambda_1) & \lambda_1\psi_n(\lambda_1) \\ \lambda_2^4\phi_n(\lambda_2) & \lambda_2^2\phi_n(\lambda_2) & \phi_n(\lambda_2) & \lambda_2^5\psi_n(\lambda_2) & \lambda_2^3\psi_n(\lambda_2) & \lambda_2\psi_n(\lambda_2) \\ \lambda_3^4\phi_n(\lambda_3) & \lambda_3^2\phi_n(\lambda_3) & \phi_n(\lambda_3) & \lambda_3^5\psi_n(\lambda_3) & \lambda_3^3\psi_n(\lambda_3) & \lambda_3\psi_n(\lambda_3) \\ \lambda_1^2\psi_n(\lambda_1) & \lambda_1^4\psi_n(\lambda_1) & \lambda_1^6\psi_n(\lambda_1) & -\lambda_1\phi_n(\lambda_1) & -\lambda_1^3\phi_n(\lambda_1) & -\lambda_1^5\phi_n(\lambda_1) \\ \lambda_2^2\psi_n(\lambda_2) & \lambda_2^4\psi_n(\lambda_2) & \lambda_2^6\psi_n(\lambda_2) & -\lambda_2\phi_n(\lambda_2) & -\lambda_2^3\phi_n(\lambda_2) & -\lambda_2^5\phi_n(\lambda_2) \\ \lambda_3^2\psi_n(\lambda_3) & \lambda_3^4\psi_n(\lambda_3) & \lambda_3^6\psi_n(\lambda_3) & -\lambda_3\phi_n(\lambda_3) & -\lambda_3^3\phi_n(\lambda_3) & -\lambda_3^5\phi_n(\lambda_3) \end{vmatrix},$$

$$\Delta b_n^{(1)} = \begin{vmatrix} \lambda_1^4\phi_n(\lambda_1) & \lambda_1^2\phi_n(\lambda_1) & \phi_n(\lambda_1) & \lambda_1^5\psi_n(\lambda_1) & \lambda_1^3\psi_n(\lambda_1) & -\lambda_1^6\phi_n(\lambda_1) \\ \lambda_2^4\phi_n(\lambda_2) & \lambda_2^2\phi_n(\lambda_2) & \phi_n(\lambda_2) & \lambda_2^5\psi_n(\lambda_2) & \lambda_2^3\psi_n(\lambda_2) & -\lambda_2^6\phi_n(\lambda_2) \\ \lambda_3^4\phi_n(\lambda_3) & \lambda_3^2\phi_n(\lambda_3) & \phi_n(\lambda_3) & \lambda_3^5\psi_n(\lambda_3) & \lambda_3^3\psi_n(\lambda_3) & -\lambda_3^6\phi_n(\lambda_3) \\ \lambda_1^2\psi_n(\lambda_1) & \lambda_1^4\psi_n(\lambda_1) & \lambda_1^6\psi_n(\lambda_1) & -\lambda_1\phi_n(\lambda_1) & -\lambda_1^3\phi_n(\lambda_1) & -\psi_n(\lambda_1) \\ \lambda_2^2\psi_n(\lambda_2) & \lambda_2^4\psi_n(\lambda_2) & \lambda_2^6\psi_n(\lambda_2) & -\lambda_2\phi_n(\lambda_2) & -\lambda_2^3\phi_n(\lambda_2) & -\psi_n(\lambda_2) \\ \lambda_3^2\psi_n(\lambda_3) & \lambda_3^4\psi_n(\lambda_3) & \lambda_3^6\psi_n(\lambda_3) & -\lambda_3\phi_n(\lambda_3) & -\lambda_3^3\phi_n(\lambda_3) & -\psi_n(\lambda_3) \end{vmatrix}, \tag{24}$$

while $b_{n+1}^{(1)}$ is obtained from $b_n^{(1)}$ by replacing n with $n + 1$.

Because of the complexity of the results, we do not discuss the asymptotic analysis of three solitons anymore. But we will explore the shapes of three-soliton solutions in different parameters. When the parameters $\lambda_1 = 5/2$, $\lambda_2 = 1/2$, and $\lambda_3 = 1/2$, we can see the overtaking elastic interactions among unidirectional bell-shaped three solitons on the vanishing background in Figures 4(a1) and 4(a2); when we choose the parameters $\lambda_1 = 2$, $\lambda_2 = 2/5$, and $\lambda_3 = 3$, the overtaking elastic interactions among unidirectional anti-bell-shaped three solitons on the vanishing background d are shown in Figures 4(b1) and 4(b2); when we choose the parameters $\lambda_1 = 5/2$, $\lambda_2 = 2$, and $\lambda_3 = 1/3$, the overtaking elastic interactions among unidirectional two bell-shaped solitons and one anti-bell-shaped soliton on the vanishing background are shown in Figures 4(c1) and 4(c2); when we choose the parameters $\lambda_1 = 2$, $\lambda_2 = 2/5$, and $\lambda_3 = 1/3$, the overtaking elastic interactions among two unidirectional anti-bell-shaped solitons and one bell-shaped soliton on the vanishing background are shown in Figures 4(d1) and 4(d2). Using the same analysis method as the high amplitude of the two-soliton solution, we can also analyze the reason for the high amplitude of the soliton in Figures 4(d1) and 4(d2) by choosing three spectral parameters λ_1, λ_2, and λ_3, so we will not do a detailed analysis here.

3.2. Discrete RS Solutions and Their Asymptotic Analysis. In this section, we will use the discrete generalized $(1, N-1)$ -fold DT to construct RS solutions with the initial nonzero constant seed solution $q_n = c$. Because of the change of the initial background, we must rewrite solution (14) as

$$\varphi_n = \begin{pmatrix} \phi_n \\ \psi_n \end{pmatrix} = \begin{pmatrix} C_1\tau_+^n e^{\rho_+ t} + C_2\tau_-^n e^{\rho_- t} \\ C_1\dfrac{\tau_+ - \lambda}{a}\tau_+ e^{\rho_1 t} + C_2\dfrac{\tau_- - \lambda}{a}\tau_- e^{\rho_- t} \end{pmatrix}, \tag{25}$$

where

$$\tau_\pm = \frac{1}{2\lambda}\left(\lambda^2 + 1 \pm \sqrt{\lambda^4 - (4c^2 + 2)\lambda^2 + 1}\right),$$

$$\rho_{\pm} = \frac{1}{2\lambda^4}\left[\left(\lambda^8 - 2\lambda^6 + 6c^4\lambda^4 - 2\lambda^2 + 1\right) \pm \left(\lambda^6 + \left(2c^2 - 1\right)\lambda^4 + \left(2c^2 - 1\right)\lambda^2 + 1\right)\sqrt{\lambda^4 - (4c^2 + 2)\lambda^2 + 1}\right], \tag{26}$$

and C_1, C_2 are arbitrary constants. Next, we fix the spectral parameter $\lambda = \lambda_1 + \varepsilon^2$ with $\lambda_1 = c + \sqrt{c^2 + 1}$. In particular, if we take $C_1 = -C_2 = 1/\varepsilon$, $c = 3/4$ and expand the vector function φ in equation (25) as two Taylor series at $\varepsilon = 0$, let $\xi = 64n + 675t$, and then, we can obtain

$$\varphi_n\left(\varepsilon^2\right) = \sum_{k=0}^{\infty} \varphi_n^{(k)}\varepsilon^{2k} = \varphi_n^{(0)} + \varphi_n^{(1)}\varepsilon^2 + \varphi_n^{(2)}\varepsilon^4 + \varphi_n^{(3)}\varepsilon^6 +, \cdots, \tag{27}$$

with

$$\varphi_n^{(0)} = \begin{pmatrix} \phi_n^{(0)} \\ \psi_n^{(0)} \end{pmatrix} = \left(\frac{5}{4}\right)^n \frac{\sqrt{15}}{160} e^{(1211/256)t} \begin{pmatrix} \xi \\ 320 - 3\xi \end{pmatrix},$$

$$\varphi_n^{(1)} = \begin{pmatrix} \phi_n^{(1)} \\ \psi_n^{(1)} \end{pmatrix} = \left(\frac{5}{4}\right)^n \frac{\sqrt{15}}{19660800} e^{(1211/256)t} \cdot \begin{pmatrix} 3\xi^3 + 1497600t\xi + 7168\xi + 125337600t \\ 3\xi^3 - 960\xi^2 + 1497600t\xi + 109568\xi - 34406400t - \dfrac{6225920}{3} \end{pmatrix},$$

$$\varphi_n^{(2)} = \begin{pmatrix} \phi_n^{(2)} \\ \psi_n^{(2)} \end{pmatrix}, \tag{28}$$

in which

$$\phi_n^{(2)} = \left(\frac{5}{4}\right)^n \frac{3\sqrt{15}e^{(1211/256)t}}{72477573120000}\left[27\xi^5 + (44928000t + 645120)\xi^3 + 11280384000\xi^2 t + \left(11214028800000t^2 + 1751777280000t - 7504658432\right)\xi + 1877055897600000t^2 + 99792558489600t\right],$$

$$\psi_n^{(2)} = \left(\frac{5}{4}\right)^n \frac{3\sqrt{15}e^{(1211/256)t}}{72477573120000}\left[81\xi^5 - 43200\xi^4 + (134784000t + 11151360)\xi^3 - (9289728000t + 973209600)\xi^2 + 20426784768600000t^2 + \left(33642086400000t^2 + 2636513280000t - 38242615296\right)\xi + 64958024908800t + 1410963865600\right], \tag{29}$$

and the rest $\varphi_n^{(j)}(j \geq 3)$ are omitted here.

(I) when N=1, we can give the first-order RS solution of equation (1) by using the discrete generalized $(1, 0)$ -fold DT as

$$\tilde{q}_n = ca_{n+1}^{(0)} + b_{n+1}^{(1)}, \tag{30}$$

where $a_n^{(0)} = \Delta a_n^{(0)}/\Delta_n$ and $b_n^{(1)} = \Delta b_n^{(1)}/\Delta_n$, in which

$$\Delta_n = \begin{vmatrix} \phi_n^{(0)}(\lambda_1) & \lambda_1\psi_n^{(0)}(\lambda_1) \\ \lambda_1^2\psi_n^{(0)}(\lambda_1) & -\lambda_1\phi_n^{(0)}(\lambda_1) \end{vmatrix},$$
$$\Delta b_n^{(1)} = \begin{vmatrix} \phi_n^{(0)}(\lambda_1) & -\lambda_1^2\phi_n^{(0)}(\lambda_1) \\ \lambda_1^2\psi_n(\lambda_1) & -\psi_n^{(0)}(\lambda_1) \end{vmatrix}, \tag{31}$$
$$\Delta a_n^{(0)} = \begin{vmatrix} -\lambda_1^2\phi_n^{(0)}(\lambda_1) & \lambda_1\psi_n^{(0)}(\lambda_1) \\ -\psi_n^{(0)}(\lambda_1) & -\lambda_1\phi_n^{(0)}(\lambda_1) \end{vmatrix},$$

while $a_{n+1}^{(0)}, b_{n+1}^{(1)}$ are obtained from $a_n^{(0)}, b_n^{(1)}$ by replacing n with $n + 1$. So just for analysis purposes, let's rewrite this solution as

$$\tilde{q}_n = \frac{3}{4} - \frac{4.6875}{\left[(3/2)(n + (675/64)t) - (1/2)\right]^2 + 1}, \tag{32}$$

from which we can conclude or infer the following physical characteristics of RS solution (32):

(i) $\tilde{q}_n \longrightarrow 3/4$ as $n \longrightarrow \pm\infty$ or $t \longrightarrow \pm\infty$, which clearly shows that the RS solution turned out to be what it was at the beginning of initial background 3/4. It is also worth to notice that $\tilde{q}_n$ reaches the minimum of −63/16 when the RS solution along the line $3\xi - 64 = 0$, namely, the amplitude of this solution is 63/16

(ii) The widths, velocities, wave number, and primary phases of this solution are 2/3, 675/64, 3/2 and −1/2, respectively

(iii) After removing the background 3/4 of solution (32), similar to the analysis of one-soliton solution (17), we can also calculate the energy $1875/256\pi$ of solution (32)

What is more, we plot its structure figures as shown in Figures 5(a1) and 5(a2).

(II) when N=2, we can give the second-order RS solution of equation (1) via the generalized $(1, 1)$-fold DT as

$$\tilde{q}_n = ca_{n+1}^{(0)} + b_{n+1}^{(1)}, \tag{33}$$

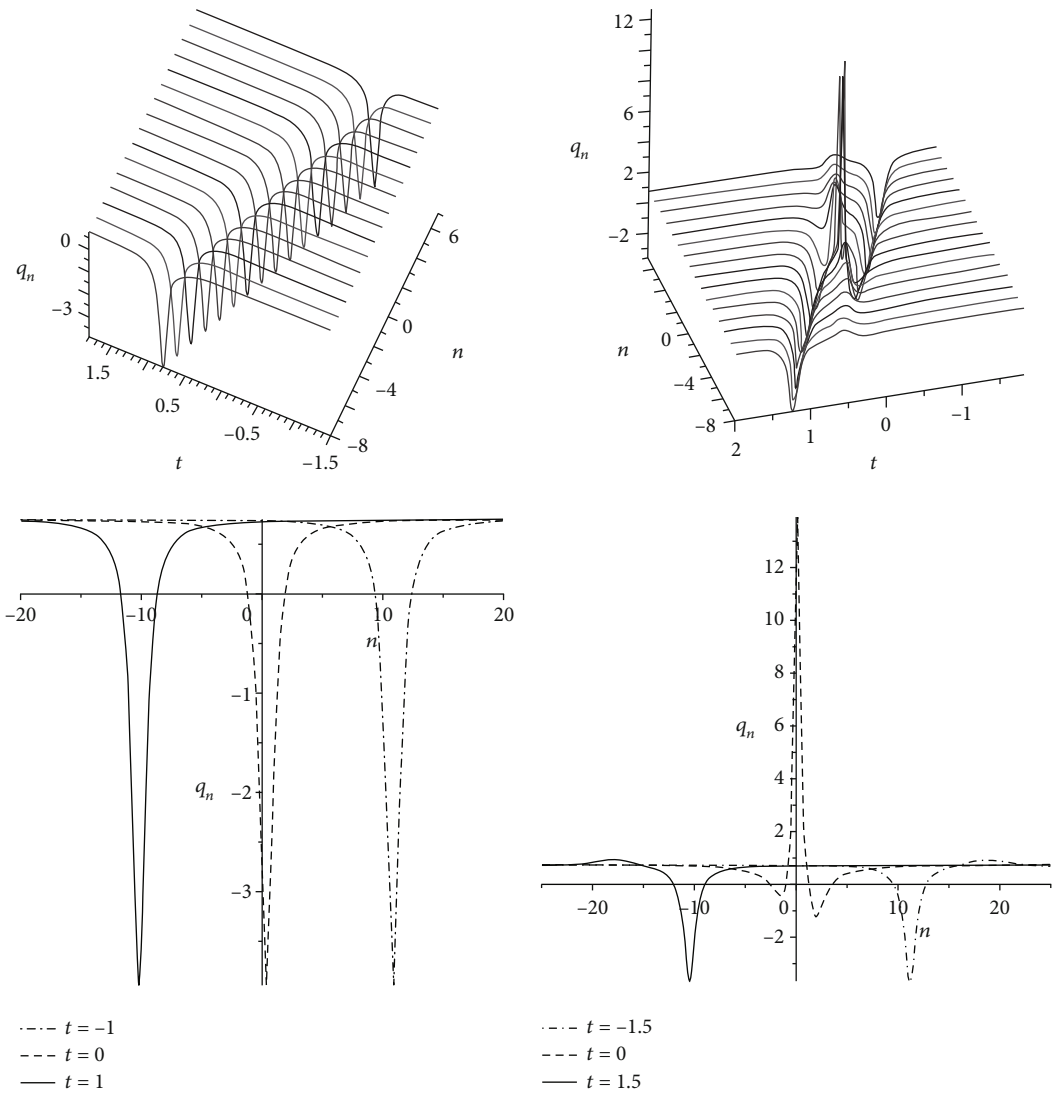

Figure 5: Continued.

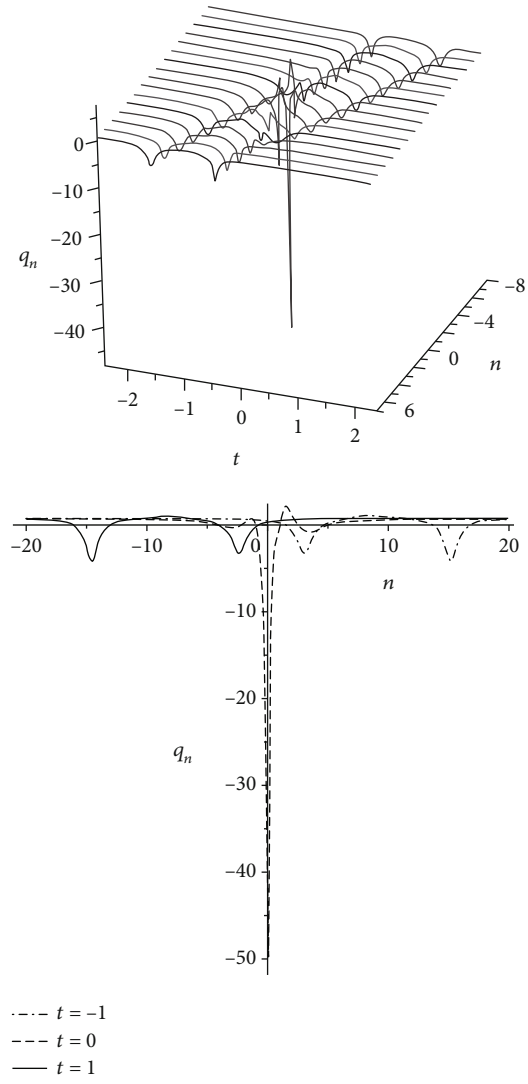

(c)

FIGURE 5: RS solution $\tilde{q}_n$ with the parameter $\lambda_1 = 2$. (a1, a2) First-order RS; (b1, b2) second-order RS; (c1, c2) third-order RS. (a2–c2) The propagation processes for $\tilde{q}_n$ at different time corresponding to (a1–c1), respectively.

where $a_n^{(0)} = \Delta a_n^{(0)}/\Delta_n$ and $b_n^{(1)} = \Delta b_n^{(1)}/\Delta_n$, in which

$$\Delta_n = \begin{vmatrix} \lambda_1^2\phi_n^{(0)} & \phi_n^{(0)} & \lambda_1^3\psi_n^{(0)} & \lambda_1\psi_n^{(0)} \\ \lambda_1^2\psi_n^{(0)} & \lambda_1^4\psi_n^{(0)} & -\lambda_1\phi_n^{(0)} & -\lambda_1^3\phi_n^{(0)} \\ \lambda_1^2\phi_n^{(1)} + 2\lambda_1\phi_n^{(0)} & \phi_n^{(1)} & \lambda_1^3\psi_n^{(1)} + 3\lambda_1^2\psi_n^{(0)} & \lambda_1\psi_n^{(1)} + \psi_n^{(0)} \\ \lambda_1^2\psi_n^{(1)} + 2\lambda_1\psi_n^{(0)} & \lambda_1^4\psi_n^{(1)} + 4\lambda_1^3\psi_n^{(0)} & -\lambda_1\phi_n^{(1)} - \phi_1^{(0)} & -\lambda_1^3\phi_n^{(1)} - 3\lambda_1^2\phi_n^{(0)} \end{vmatrix},$$

$$\Delta a_n^{(0)} = \begin{vmatrix} \lambda_1^2\phi_n^{(0)} & \phi_n^{(0)} & -\lambda_1^4\phi_n^{(0)} & \lambda_1\psi_n^{(0)} \\ \lambda_1^2\psi_n^{(0)} & -\psi_n^{(0)} & -\lambda_1\phi_n^{(0)} & -\lambda_1^3\phi_n^{(0)} \\ \lambda_1^2\phi_n^{(1)} + 2\lambda_1\phi_n^{(0)} & -\lambda^4\phi_n^{(1)} - 4\lambda^3\phi_n^{(0)} & \lambda_1^3\psi_n^{(1)} + 3\lambda_1^2\psi_n^{(0)} & \lambda_1\psi_n^{(1)} + \psi_n^{(0)} \\ \lambda_1^2\psi_n^{(1)} + 2\lambda_1\psi_n^{(0)} & -\psi_n^{(1)} & -\lambda_1\phi_n^{(1)} - \phi_1^{(0)} & -\lambda_1^3\phi_n^{(1)} - 3\lambda_1^2\phi_n^{(0)} \end{vmatrix}, \tag{34}$$

$$\Delta b_n^{(1)} = \begin{vmatrix} \lambda_1^2\phi_n^{(0)} & \phi_n^{(0)} & \lambda_1^3\psi_n^{(0)} & -\lambda_1^4\phi_n^{(0)} \\ \lambda_1^2\psi_n^{(0)} & \lambda_1^4\psi_n^{(0)} & -\lambda_1\phi_n^{(0)} & -\psi_n^{(0)} \\ \lambda_1^2\phi_n^{(1)} + 2\lambda_1\phi_n^{(0)} & \phi_n^{(1)} & \lambda_1^3\psi_n^{(1)} + 3\lambda_1^2\psi_n^{(0)} & -\lambda^4\phi_n^{(1)} - 4\lambda^3\phi_n^{(0)} \\ \lambda_1^2\psi_n^{(1)} + 2\lambda_1\psi_n^{(0)} & \lambda_1^4\psi_n^{(1)} + 4\lambda_1^3\psi_n^{(0)} & -\lambda_1\phi_n^{(1)} - \phi_1^{(0)} & -\psi_n^{(1)} \end{vmatrix}.$$

For the sake of discussion, the simplification form of solution (33) is listed as follows:

$$\tilde{q}_n = \frac{3}{4} + \frac{F}{G}, \tag{35}$$

where

$$\begin{aligned} F = {} & -34789235097600n^4 + (-1467670855680000t - 185542587187200)n^3 \\ & + (-23219011584000000t^2 - 5870683422720000t - 429067232870400)n^2 \\ & + (-1632586752000000000t^3 - 61917364224000000t^2 \\ & - 14595171287040000t - 432932703436800)n - 430467210000000000t^4 \\ & - 217678233600000000t^3 - 106205478912000000t^2 \\ & - 11958799564800000t - 77309411328000, \end{aligned}$$

$$\begin{aligned} G = {} & 5566277615616n^6 + (352241005363200t + 44530220924928)n^5 \\ & + (9287604633600000t^2 + 2348273369088000t \\ & + 144723218006016)n^4 + (130606940160000000t^3 \\ & + 49533891379200000t^2 + 5218385264640000t + 252337918574592)n^3 \\ & + (1033121304000000000t^4 + 522427760640000000t^3 \\ & + 68521883074560000t^2 + 4435627474944000t + 307382219440128)n^2 \\ & + (4358480501250000000t^5 + 2754990144000000000t^4 \\ & + 383113691136000000t^3 + 9356401704960000t^2 \\ & + 3822467206348800t + 263882790666240)n + 7661391506103515625t^6 \\ & + 5811307335000000000t^5 + 749969539200000000t^4 \\ & - 98680799232000000t^3 + 41469345792000000t^2 \\ & + 2783138807808000t + 109951162777600. \end{aligned} \tag{36}$$

In order to understand the physical properties of the second-order RS solution of equation (1) better, we can still perform the asymptotic analysis. For convenience, let $\zeta = 64n + 675t - 64(1275/16)^{1/3}t^{1/3}$; we can calculate the limits of $\tilde{q}_n$ in (35), which only gives the following one limiting state when $t \longrightarrow \pm\infty$:

$$\tilde{q}_n \longrightarrow q^{\pm} = \frac{3}{4} - \frac{76800}{(3\zeta - 64)^2 + 16384}, (t \longrightarrow \pm\infty). \tag{37}$$

From the above calculation, we can see that $q_n^{\pm}$ is the result of $\tilde{q}_n$ when t approaches infinity and it is worth noticing that the result of positive infinity is the same as that of negative infinity. Meanwhile, the asymptotic expression (37) clearly shows that the dark RS solution $q_n^{\pm}$ reaches the minimum of $-63/16$ along the curve $3\zeta - 64 = 0$. The structures of second-order RS solution are shown in Figures 5(b1) and 5(b2), from which we can see that they are consistent with the above analysis results.

(III) when N=3, we can give the discrete third-order RS solution of equation (1) via the generalized $(1, 2)$ -fold DT as

$$\tilde{q}_n = ca_{n+1}^{(0)} + b_{n+1}^{(1)}, \tag{38}$$

where $a_n^{(0)} = \Delta a_n^{(0)}/\Delta_n$ and $b_n^{(1)} = \Delta b_n^{(1)}/\Delta_n$, in which

$$\Delta_n = \begin{vmatrix} \lambda_1^4\phi_n^{(0)} & \lambda_1^2\phi_n^{(0)} & \phi_n^{(0)} & \lambda_1^5\psi_n^{(0)} & \lambda_1^3\psi_n^{(0)} & \lambda_1\psi_n^{(0)} \\ \lambda_1^2\psi_n^{(0)} & \lambda_1^4\psi_n^{(0)} & \lambda_1^6\psi_n^{(0)} & -\lambda_1\phi_n^{(0)} & -\lambda_1^3\phi_n^{(0)} & -\lambda_1^5\phi_n^{(0)} \\ \Delta^{(3,1)} & \Delta^{(3,2)} & \phi_n^{(1)} & \Delta^{(3,4)} & \Delta^{(3,5)} & \Delta^{(3,6)} \\ \Delta^{(4,1)} & \Delta^{(4,2)} & \Delta^{(4,3)} & \Delta^{(4,4)} & \Delta^{(4,5)} & \Delta^{(4,6)} \\ \Delta^{(5,1)} & \Delta^{(5,2)} & \phi_n^{(2)} & \Delta^{(5,4)} & \Delta^{(5,5)} & \Delta^{(5,6)} \\ \Delta^{(6,1)} & \Delta^{(6,2)} & \Delta^{(6,3)} & \Delta^{(6,4)} & \Delta^{(6,5)} & \Delta^{(6,6)} \end{vmatrix},$$

$$\Delta a_n^{(0)} = \begin{vmatrix} \lambda_1^4\phi_n^{(0)} & \lambda_1^2\phi_n^{(0)} & -\lambda_1^6\phi_n^{(0)} & \lambda_1^5\psi_n^{(0)} & \lambda_1^3\psi_n^{(0)} & \lambda_1\psi_n^{(0)} \\ \lambda_1^2\psi_n^{(0)} & \lambda_1^4\psi_n^{(0)} & -\psi_n^{(0)} & -\lambda_1\phi_n^{(0)} & -\lambda_1^3\phi_n^{(0)} & -\lambda_1^5\phi_n^{(0)} \\ \Delta^{(3,1)} & \Delta^{(3,2)} & -\lambda_1^6\phi_n^{(1)} - 6\lambda_1^5\phi_n^{(0)} & \Delta^{(3,4)} & \Delta^{(3,5)} & \Delta^{(3,6)} \\ \Delta^{(4,1)} & \Delta^{(4,2)} & -\psi_n^{(1)} & \Delta^{(4,4)} & \Delta^{(4,5)} & \Delta^{(4,6)} \\ \Delta^{(5,1)} & \Delta^{(5,2)} & -\lambda_1^6\phi_n^{(2)} - 6\lambda_1^5\phi_n^{(1)} - 15\lambda_1^{(4)}\phi_n^{(0)} & \Delta^{(5,4)} & \Delta^{(5,5)} & \Delta^{(5,6)} \\ \Delta^{(6,1)} & \Delta^{(6,2)} & -\psi_n^{(2)} & \Delta^{(6,4)} & \Delta^{(6,5)} & \Delta^{(6,6)} \end{vmatrix},$$

$$\Delta b_n^{(1)} = \begin{vmatrix} \lambda_1^4\phi_n^{(0)} & \lambda_1^2\phi_n^{(0)} & \phi_n^{(0)} & \lambda_1^5\psi_n^{(0)} & \lambda_1^3\psi_n^{(0)} & -\lambda_1^6\phi_n^{(0)} \\ \lambda_1^2\psi_n^{(0)} & \lambda_1^4\psi_n^{(0)} & \lambda_1^6\psi_n^{(0)} & -\lambda_1\phi_n^{(0)} & -\lambda_1^3\phi_n^{(0)} & -\psi_n^{(0)} \\ \Delta^{(3,1)} & \Delta^{(3,2)} & \phi_n^{(1)} & \Delta^{(3,4)} & \Delta^{(3,5)} & -\lambda_1^6\phi_n^{(1)} - 6\lambda_1^5\phi_n^{(0)} \\ \Delta^{(4,1)} & \Delta^{(4,2)} & \Delta^{(4,3)} & \Delta^{(4,4)} & \Delta^{(4,5)} & -\psi_n^{(1)} \\ \Delta^{(5,1)} & \Delta^{(5,2)} & \phi_n^{(2)} & \Delta^{(5,4)} & \Delta^{(5,5)} & -\lambda_1^6\phi_n^{(2)} - 6\lambda_1^5\phi_n^{(1)} - 15\lambda_1^{(4)}\phi_n^{(0)} \\ \Delta^{(6,1)} & \Delta^{(6,2)} & \Delta^{(6,3)} & \Delta^{(6,4)} & \Delta^{(6,5)} & -\psi_n^{(2)} \end{vmatrix}, \tag{39}$$

with

$$\Delta^{(3,1)} = \lambda_1^4\phi_n^{(1)} + 4\lambda_1^3\phi_n^{(0)},$$

$$\Delta^{(3,2)} = \lambda_1^2\phi_n^{(1)} + 2\lambda_1\phi_n^{(0)},$$

$$\Delta^{(3,4)} = \lambda_1^5\psi_n^{(1)} + 5\lambda_1^4\psi_n^{(0)},$$

$$\Delta^{(3,5)} = \lambda_1^3\psi_n^{(1)} + 3\lambda_1^2\psi_n^{(0)},$$

$$\Delta^{(3,6)} = \lambda_1\psi_n^{(1)} + \psi_n^{(0)},$$

$$\Delta^{(4,1)} = \lambda_1^2\psi_n^{(1)} + 2\lambda_1\psi_n^{(0)},$$

$$\Delta^{(4,2)} = \lambda_1^4\psi_n^{(1)} + 4\lambda_1^3\psi_n^{(0)},$$

$$\Delta^{(4,3)} = \lambda_1^6\psi_n^{(1)} + 6\lambda_1^5\psi_n^{(0)},$$

$$\Delta^{(4,4)} = -\lambda_1\phi_n^{(1)} - \phi_1^{(0)},$$

$$\Delta^{(4,5)} = -\lambda_1^3\phi_n^{(1)} - 3\lambda_1^2\phi_n^{(0)},$$

$$\Delta^{(4,6)} = -\lambda_1^5\phi_n^{(1)} - 5\lambda_1^4\phi_n^{(0)},$$

$$\Delta^{(5,1)} = \lambda_1^4\phi_n^{(2)} + 4\lambda_1^3\phi_n^{(1)} + 6\lambda_1^2\phi_n^{(0)},$$

$$\Delta^{(5,2)} = \lambda_1^2\phi_n^{(2)} + 2\lambda_1\phi_n^{(1)} + \phi_n^{(0)},$$

$$\Delta^{(5,4)} = \lambda_1^5\psi_n^{(2)} + 5\lambda_1^4\psi_n^{(1)} + 10\lambda_1^3\psi_n^{(0)},$$

$$\Delta^{(5,5)} = \lambda_1^3\psi_n^{(2)} + 3\lambda_1^2\psi_n^{(1)} + 3\lambda_1\psi_n^{(0)},$$

$$\Delta^{(5,6)} = \lambda_1\psi_n^{(2)} + \psi_n^{(1)},$$

$$\Delta^{(6,1)} = \lambda_1^2\psi_n^{(2)} + 2\lambda_1\psi_n^{(1)} + \psi_n^{(0)},$$

$$\Delta^{(6,2)} = \lambda_1^4\psi_n^{(2)} + 4\lambda_1^3\psi_n^{(1)} + 6\lambda_1^2\psi_n^{(0)},$$

$$\Delta^{(6,3)} = \lambda_1^6\psi_n^{(2)} + 6\lambda_1^5\psi_n^{(1)} + 15\lambda_1^4\psi_n^{(0)},$$

$$\Delta^{(6,4)} = -\lambda_1\phi_n^{(2)} - \phi_n^{(1)},$$

$$\Delta^{(6,5)} = -\lambda_1^3\phi_n^{(2)} - 3\lambda_1^2\phi_n^{(1)} - 3\lambda_1\phi_n^{(0)},$$

$$\Delta^{(6,6)} = -\lambda_1^5\phi_n^{(2)} - 5\lambda_1^4\phi_n^{(1)} - 10\lambda_1^3\phi_n^{(0)}. \tag{40}$$

The simplification form of solution (38) can be also calculated by using symbolic computation. But it is so complicated that therefore, we omit it here. Besides, the asymptotic analysis can be still performed. Similar to the above analysis process of second-order RS, let $\zeta_1 = 64n + 675t - 64((6375/32) + ((3825\sqrt{5})/32))^{1/3}t^{1/3}$, $\zeta_2 = 64n + 675t - 64((6375/32) + ((3825\sqrt{5})/32))^{1/3}t^{1/3}$, and $b = ((6375/32) + ((3825\sqrt{5})/32))^{1/3} - ((6375/32) + ((3825\sqrt{5})/32))^{1/3}$; then, it turns out that solutions $\tilde{q}_n$ have two different asymptotic states when $|t| \longrightarrow \infty$:

(i) If $\zeta_1 = 64n + 675t - 64((6375/32) + ((3825\sqrt{5})/32))^{1/3}t^{1/3} = O(1)$, from $\zeta_2 = \zeta_1 - bt^{1/3}$, we can get $\zeta_2 \longrightarrow \pm\infty$ as $t \longrightarrow \mp\infty$; then, calculating the limit of solution $\tilde{q}_n$ in (38) gives the following asymptotic state expression in the form

$$\tilde{q}_n \longrightarrow q_1^{\pm} = \frac{3}{4} - \frac{76800}{(3\zeta_1 - 64)^2 + 16384}, \quad \left(bt^{\frac{1}{3}} \longrightarrow \pm\infty\right). \tag{41}$$

(ii) If $\zeta_2 = 64n + 675t - 64((6375/32) + ((3825\sqrt{5})/32))^{1/3}t^{1/3} = O(1)$, from $\zeta_1 = \zeta_2 + bt^{1/3}$, we can get $\zeta_1 \longrightarrow \pm\infty$ as $t \longrightarrow \pm\infty$; then, calculating the limit of solution $\tilde{q}_n$ in (38) gives the following asymptotic state expression as

$$\tilde{q}_n \longrightarrow q_2^{\pm} = \frac{3}{4} - \frac{76800}{(3\zeta_2 - 64)^2 + 16384}, \quad \left(bt^{\frac{1}{3}} \longrightarrow \pm\infty\right). \tag{42}$$

From the above calculation, we can see that $q_1^{\pm}$ and $q_2^{\pm}$ are the two results of $\tilde{q}_n$ when t approaches infinity and $3\zeta_1 - 64 = 0$ and $3\zeta_2 - 64 = 0$ are also the two center trajectories of solution $\tilde{q}_n$. Meanwhile, the form of the third-order

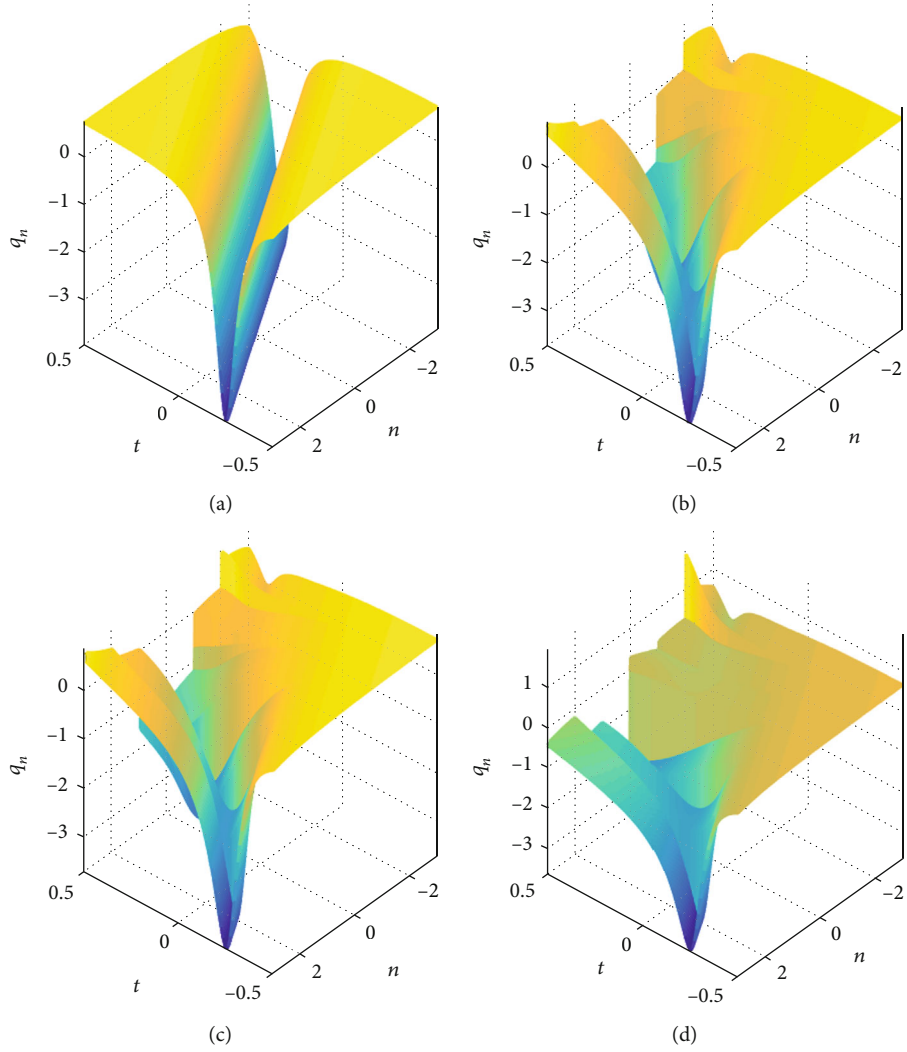

FIGURE 6: One-order RS (32) with the same parameters as in Figure 5 (a) RS solutions; (b) time evolutions without small noise; (c) time evolutions with 0.01% noise; (d) time evolutions with 0.05% noise.

RS solution at infinity clearly shows that $q_1^{\pm}$ and $q_2^{\pm}$ reach the minimum along curves $3\zeta_1 - 64 = 0$ and $3\zeta_2 - 64 = 0$, respectively. The structure of the third-order RS solution is shown in Figures 5(c1) and 5(c2), which is consistent with the result of above analysis.

Remark 3. The point here is that when we perform asymptotic analysis to the usual two-soliton and three-soliton solutions, the final two and three solitons keep their shape before and after the collisions, and for asymptotic analysis to second-order and third-order RS solutions, we find that there is one first-order RS left at infinity for second-order RS solutions and the other first-order RS disappears at infinity, while there are two first-order RSs left at infinity for third-order RS solutions and the third RS disappears. For higher-order RS solutions, there is always a RS solution that disappears at infinity, which is a little like rogue wave solutions that are asymptotic to the background wave at infinity, and we find that these new phenomena about RS are interesting and quite different from those of the USs, which is worthy of further investigation.

Similar to numerical simulation of the usual one-soliton solution in the previous subsection, we can also add the perturbations to RS solutions in order to show its dynamical behavior and propagation stability. Figure 6 shows first-order RS solution (32) of equation (1), time evolutions of using first-order RS solution (32), and time evolutions of adding 0.01% and 0.05% perturbations to first-order RS solution (32). As can be seen, Figures 6(a) and 6(b) show that the representation of time evolutions for solution (32) without noise is nearly close to first-order RS solution (32) in time $t \in (-0.5, 0.5)$, which shows the accuracy of our numerical scheme. However, as time goes on, even without noise, there is a large fluctuation. Different from the usual one-soliton solution, Figures 6(c) and 6(d) exhibit that the evolutions of wave propagation perform the relatively large oscillations with the increase of time t if we add 0.01% and 0.05% perturbations to the initial solutions. We find that

Table 4: Main mathematical features of rational solutions $\tilde{q}_n$ of order N.

N	Background	Highest powers in the numerator	Highest powers in the denominator
1	3/4	2	2
2	3/4	6	6
3	3/4	12	12
…	…	…	…
N	3/4	$N(N+1)$	$N(N+1)$

the first-order RS is more sensitive to a very small noise than the usual one-soliton solution. So, we can conclude that the evolution behavior of the first-order RS solution is unstable even at a very small noise, that is to say that the RS solution is weaker than the US against small noise. This phenomenon also exists for higher-order RS solutions, which will not be discussed here.

Finally, when $N \geq 4$, we also discuss higher-order RS solutions, which are very complicated, and we will not discuss them here. Some mathematical features of rational solution $\tilde{q}_n$ for equation (1) are summarized in Table 4. It is worth noting that the first column in Table 4 means the order number of RS solutions and the second column represents the background levels of RS solutions, while the third and fourth columns exhibit the highest powers in the numerator and denominator of the polynomials involved in each RS solution, respectively.

3.3. Discrete Mixed Soliton Solutions and Their Asymptotic Analysis. In the previous contents, we have used the discrete N-fold DT with N spectral parameters to explore the US solutions and then used discrete generalized $(1, N-1)$-fold DT with only one spectral parameter to explore RS solutions. In this section, we will use the discrete generalized $(2, N-2)$-fold DT to construct mixed soliton solutions of equation (1) with its initial nonzero solution $q_n = a$. In the following, we only discuss the case $N = 2$. Besides, we also will use symbolic computation and asymptotic analysis to discuss the interaction phenomena of US and RS. When $N = 2$, we fix the spectral parameters in equation (25) as $\lambda_1 = \lambda_1 + \varepsilon^2$ and $\lambda_2 = 3$ with $\lambda_1 = c + \sqrt{c^2+1}$. In particular, we will get the same form of Taylor series (27) if we take $c = 3/4$ and expand the vector function φ_n in equation (25). Besides, when we choose $C_1 = C_2 = 1$ in equation (25), the mixed interaction solution of the usual one-soliton and first-order RS of equation (1) can be given as

$$\tilde{q}_n = c a_{n+1}^{(0)} + b_{n+1}^{(1)}, \tag{43}$$

where $a_n^{(0)}$ and $b_n^{(1)}$ can be determined by the following system:

$$\begin{aligned} T_n^{(0)}(\lambda_1)\varphi_n^{(0)}(\lambda_1) &= 0, \\ T_n(\lambda_2)\varphi_n(\lambda_2) &= 0, \end{aligned} \tag{44}$$

with $a_n^{(0)} = \Delta a_n^{(0)}/\Delta_n$ and $b_n^{(1)} = \Delta b_n^{(1)}/\Delta_n$, in which

$$\begin{aligned}
\Delta_n &= \begin{vmatrix} \lambda_1^2\phi_n^{(0)}(\lambda_1) & \phi_n^{(0)}(\lambda_1) & \lambda_1^3\psi_n^{(0)}(\lambda_1) & \lambda_1\psi_n^{(0)}(\lambda_1) \\ \lambda_2^2\phi_n(\lambda_2) & \psi_n(\lambda_2) & \lambda_2^3\psi_n(\lambda_2) & \lambda_2\psi_n(\lambda_2) \\ \lambda_1^2\psi_n^{(0)}(\lambda_1) & \lambda_1^4\psi_n^{(0)}(\lambda_1) & -\lambda_1\phi_n^{(0)}(\lambda_1) & -\lambda_1^3\phi_n^{(0)}(\lambda_1) \\ \lambda_2^2\psi_n(\lambda_2) & \lambda_2^4\psi_n(\lambda_2) & -\lambda_2\phi_n(\lambda_2) & -\lambda_2^3\phi_n(\lambda_2) \end{vmatrix}, \\
\Delta a_n^{(0)} &= \begin{vmatrix} \lambda_1^2\phi_n^{(0)}(\lambda_1) & -\lambda_1^4\phi_n^{(0)}(\lambda_1) & \lambda_1^3\psi_n^{(0)}(\lambda_1) & \lambda_1\psi_n^{(0)}(\lambda_1) \\ \lambda_2^2\phi_n(\lambda_2) & -\lambda_2^4\phi_n(\lambda_2) & \lambda_2^3\psi_n(\lambda_2) & \lambda_2\psi_n(\lambda_2) \\ \lambda_1^2\psi_n^{(0)}(\lambda_1) & -\psi_n^{(0)}(\lambda_1) & -\lambda_1\phi_n^{(0)}(\lambda_1) & -\lambda_1^3\phi_n^{(0)}(\lambda_1) \\ \lambda_2^2\psi_n(\lambda_2) & -\psi_n(\lambda_2) & -\lambda_2\phi_n(\lambda_2) & -\lambda_2^3\phi_n(\lambda_2) \end{vmatrix}, \\
\Delta b_n^{(1)} &= \begin{vmatrix} \lambda_1^2\phi_n^{(0)}(\lambda_1) & \phi_n^{(0)}(\lambda_1) & \lambda_1^3\psi_n^{(0)}(\lambda_1) & -\lambda_1^4\phi_n^{(0)}(\lambda_1) \\ \lambda_2^2\phi_n(\lambda_2) & \psi_n(\lambda_2) & \lambda_2^3\psi_n(\lambda_2) & -\lambda_2^4\phi_n(\lambda_2) \\ \lambda_1^2\psi_n^{(0)}(\lambda_1) & \lambda_1^4\psi_n^{(0)}(\lambda_1) & -\lambda_1\phi_n^{(0)}(\lambda_1) & -\psi_n^{(0)}(\lambda_1) \\ \lambda_2^2\psi_n(\lambda_2) & \lambda_2^4\psi_n(\lambda_2) & -\lambda_2\phi_n(\lambda_2) & -\psi_n(\lambda_2) \end{vmatrix}. \end{aligned} \tag{45}$$

With the aid of symbolic computation, solution (43) of equation (1) can be exactly expressed as

$$\tilde{q}_n = \frac{3}{4} + \frac{F}{G}, \tag{46}$$

where

$$\begin{aligned}
F = {} & -8601600\left(\frac{575}{9} - \frac{200\sqrt{7}}{9}\right)^n \left(\sqrt{7} + \frac{29}{4}\right) e^{-((14825t\sqrt{7})/648)} \\
& + 8601600\left(\sqrt{7} - \frac{29}{4}\right)\left(\frac{575}{9} + \frac{200\sqrt{7}}{9}\right)^n e^{((14825t\sqrt{7})/648)} \\
& + 135475200 \cdot 25^n \left(n^2 + \frac{675}{32}nt + \frac{8}{3}n + \frac{455625}{4096}t^2 + \frac{225}{8}t + \frac{361}{126}\right), \\
G = {} & 4128768\left(\frac{575}{9} - \frac{200\sqrt{7}}{9}\right)^n \left(\sqrt{7}n^2 + \frac{675\sqrt{7}nt}{32} + \frac{230\sqrt{7}n}{21}\right. \\
& + \frac{455625\sqrt{7}t^2}{4096} + \frac{25875\sqrt{7}t}{224} + \frac{140\sqrt{7}}{9} + \frac{29n^2}{4} + \frac{19575nt}{128} \\
& \left. + \frac{82n}{3} + \frac{13213125t^2}{16384} + \frac{9225t}{32} + \frac{2731}{63}\right) e^{-((14825t\sqrt{7})/648)} \\
& - 4128768\left(\frac{575}{9} + \frac{200\sqrt{7}}{9}\right)^n \left(\sqrt{7}n^2 + \frac{675\sqrt{7}nt}{32} + \frac{230\sqrt{7}n}{21}\right. \\
& + \frac{455625\sqrt{7}t^2}{4096} + \frac{25875\sqrt{7}t}{224} + \frac{140\sqrt{7}}{9} - \frac{29n^2}{4} - \frac{19575nt}{128} \\
& \left. - \frac{82n}{3} - \frac{13213125t^2}{16384} - \frac{9225t}{32} - \frac{2731}{63}\right) e^{((14825t\sqrt{7})/648)} \\
& + 41803776 \cdot 25^n \left(n^2 + \frac{675}{32}nt + \frac{8}{3}n + \frac{455625t^2}{4096} + \frac{225t}{8} - \frac{116}{63}\right).
\end{aligned} \tag{47}$$

Before that, we have analyzed the physical shapes and properties of US and RS solutions by using asymptotic analysis. Next, we will also discuss the mixed soliton solution

Table 5: Physical characteristics of mixed solution.

Solitons	Amplitudes	Widths	Velocities	Wave number	Primary phases	Energies
$q_1^{\pm}$	77/36	$225/\left(575+20\sqrt{7}\right)$	$\left(74125\sqrt{7}\right)/\left(8280+288\sqrt{7}\right)$	$\left(575+20\sqrt{7}\right)/225$	$\ln\left(\left(29-4\sqrt{7}\right)/27\right)$	$E2/E1$
q_2^{-}	63/16	$1/\left(192\sqrt{7}\right)$	675/64	$192\sqrt{7}$	$768+256\sqrt{7}$	$1875\pi/256$
q_2^{+}	63/16	$1/\left(192\sqrt{7}\right)$	675/64	$192\sqrt{7}$	$768-256\sqrt{7}$	$1875\pi/256$

$E2=(1786875\sqrt{7}-3045000)\arctan 3\sqrt{7}+2030000\sqrt{7}-8338750$ and $E1=324(4\sqrt{7}-29)^2\ln(575-20\sqrt{7})/1457$.

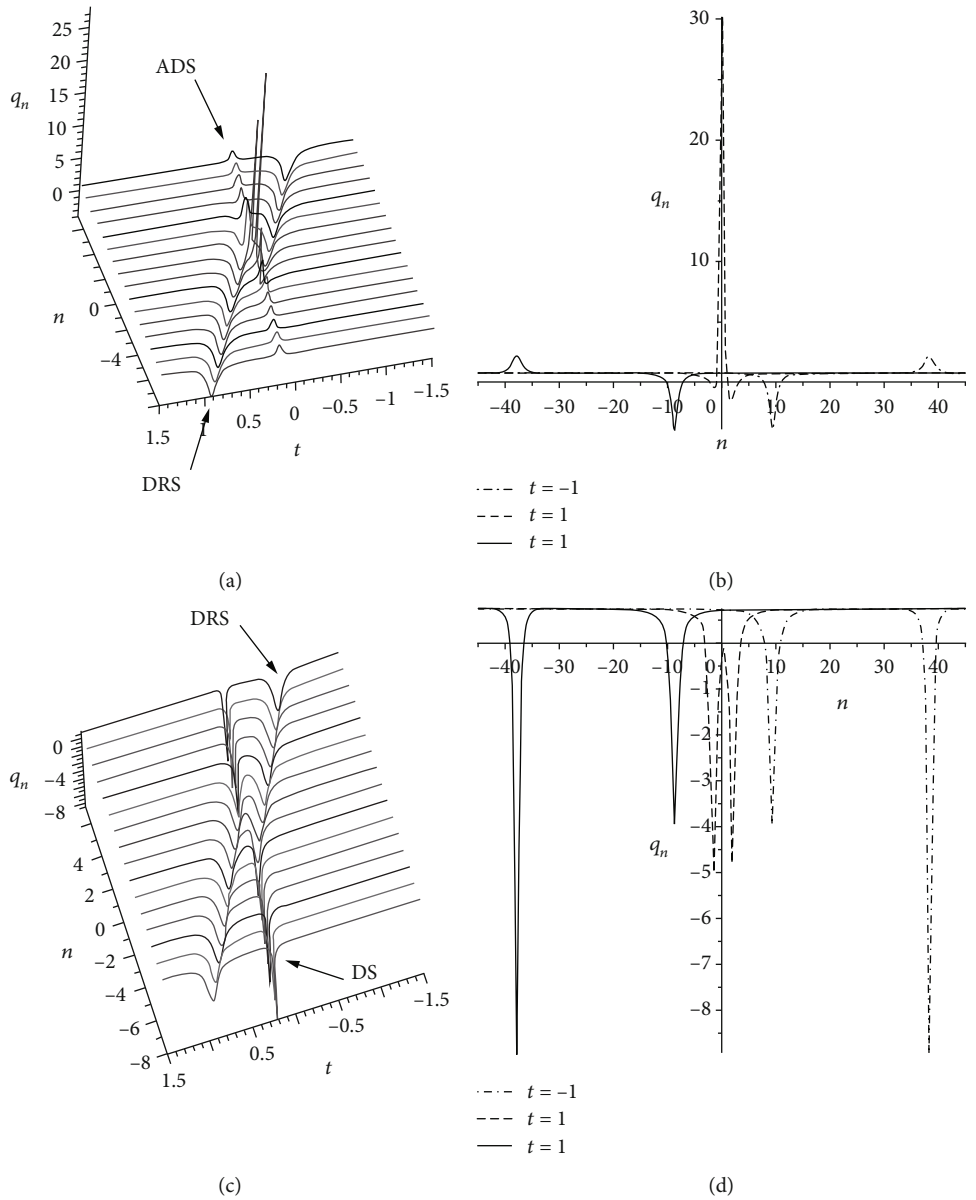

Figure 7: Mixed interaction between usual one-soliton and first-order RS of solution $\tilde{q}_n$ in (43) or (46). (a) Mixed interaction solution of one ADS and first-order DRS with parameters $\lambda_1=2,\lambda_2=3,C_1=-C_2=1$. (c) Mixed interaction solution of one DS and first-order DRS with parameters $\lambda_1=2,\lambda_2=3,C_1=C_2=1$. (b, d) The propagation processes for $\tilde{q}_n$ at $t=-1$ (solid line), $t=0$ (longdash line), and $t=1$ (dashdot line) corresponding to (a) and (c). The phrase DS stands for the usual dark soliton; the phrase ADS stands for the usual antidark soliton; the phrase DRS stands for dark one-order RS.

before and after the interaction via asymptotic analysis. Different from the previous discussion, we make appropriate variable substitution and deformation for the mixed solution in solution (43) or (46). For convenience, let $\varsigma_1 = \ln((575 + 20\sqrt{7})/225)n + ((14825t\sqrt{7})/648)t$ and $\varsigma_2 = 64n + 675t$; then, it turns out that solution $\tilde{q}_n$ has the following different asymptotic state expression when $|t| \longrightarrow \infty$:

(i) If $\varsigma_1 = O(1)$, we can get $\varsigma_2 \longrightarrow \pm\infty$ as $t \longrightarrow \pm\infty$; then, calculating the limit of solution $\tilde{q}_n$ in (43) or (46) gives the following asymptotic expressions in the form:

(i) Before and after interactions $(t \longrightarrow \pm\infty)$

$$\tilde{q}_n \longrightarrow q_1^{\pm} = \frac{3}{4} + \frac{175}{72\cos h\left[\varsigma_1 + \ln\left(\left(29 - 4\sqrt{7}\right)/27\right)\right] + 54}, \quad (\varsigma_1 \longrightarrow 0, \varsigma_2 \longrightarrow \pm\infty). \tag{48}$$

From which, we can see that the asymptotic expression $q_1^{\pm}$ displays the US structure which reaches the maximum 77/36 along the line $\varsigma_1 + \ln((29 - 4\sqrt{7})/27) = 0$. More physical characteristics of the US structure are listed in Table 5.

(ii) If $\varsigma_2 = O(1)$, we can get $\varsigma_1 \longrightarrow \pm\infty$ as $t \longrightarrow \pm\infty$; then, calculating the limit of solution $\tilde{q}_n$ in (43) or (46) gives the following asymptotic expressions in the form

(iii) Before the interaction $(t \longrightarrow -\infty)$,

$$\tilde{q}_n \longrightarrow q_2^{-} = \frac{3}{4} - \frac{537600}{63\left(\varsigma_2 + \left(\left(4608\sqrt{7} + 10752\right)/126\right)\right)^2 + 114688} \tag{49}$$

(iv) After the interaction $(t \longrightarrow +\infty)$,

$$\tilde{q}_n \longrightarrow q_2^{+} = \frac{3}{4} - \frac{537600}{63\left(\varsigma_2 - \left(\left(4608\sqrt{7} + 10752\right)/126\right)\right)^2 + 114688}. \tag{50}$$

According to the above analysis, we find that mixed soliton solution (46) possesses the following propagation characteristics and interaction properties: (i) the amplitudes, velocities, and energies of the mixed US-RS solution remain unchanged before and after the interactions; (ii) after the interactions of US and RS, the phase shift of US is zero, whereas the phase shift of RS is $-512\sqrt{7}$, that is to say that, in the mixed soliton interaction, only RS has a phase shift but US has no phase shift; (iii) the asymptotic expression $q_2^{\pm}$ displays that the RS structure reaches the minimum 63/16 along the two lines $\varsigma_2 \mp ((4608\sqrt{7} + 10752)/126) = 0$; and (iv) the relevant physical quantities of mixed soliton solution are listed in Table 5.

For solution (43) or (46), we can see that mixed soliton solution $\tilde{q}_n$ has three center trajectories and US is along one trajectory $\varsigma_1 + \ln(27/(29 + 4\sqrt{7})) = 0$, whereas RS is along two trajectories $\varsigma_2 \mp (4608\sqrt{7} \mp 10752)/126 = 0$. The structures of mixed soliton solutions are shown in Figure 7, which is consistent with our analysis above.

4. Conclusions

In this paper, we have researched the discrete mKdV equation (1), which may be used for understanding some physical phenomena such as dynamics of anharmonic lattices, solitary waves in dusty plasmas, and fluctuations in nonlinear optics. Various kinds of soliton solutions, like US, RS, and their mixed interaction soliton solutions, have been analytically investigated and discussed, which might help to understand the abovementioned physics phenomena. We sum up the main achievement of this paper as follows: firstly, we have established the generalized $(m, N-m)$-fold DT of equation (1) for the first time. Meanwhile, various kinds of soliton solutions such as US, RS, and their mixed interaction soliton solutions have been obtained via the generalized $(m, N-m)$-fold DT by choosing different values of the number m of spectral parameter λ. More importantly, asymptotic analysis has been used to analyze the limit state expressions of US, RS, and their mixed soliton solutions for equation (1). And the propagation and interaction structures between/among different types of soliton solutions have been discussed graphically. Besides, numerical simulations have been used to explore the dynamical behaviors of the US and RS solutions. Finally, some important physical quantities of US solutions, mathematical features of RS solutions, and physical quantities of mixed solutions to equation (1) have been summarized in Tables 1–5.

We hope that these results given in this paper will be helpful for understanding such physical phenomena in nonlinear optics, anharmonic lattice dynamics, and plasma environments.

Data Availability

The datasets used to support the findings of this study are included within the article.

Conflicts of Interest

The authors declare that there are no conflicts of interest regarding the publication of this paper.

Acknowledgments

This work has been partially supported by the National Natural Science Foundation of China under Grant no. 12071042 and Beijing Natural Science Foundation under Grant no. 1202006. M. L. Qin is supported by the postgraduate science and technology innovation project of Beijing Information Science and Technology University under Grant no. 5112111017.

References

[1] W. Q. Peng, S. F. Tian, and T. T. Zhang, "Breather waves, high-order rogue waves and their dynamics in the coupled nonlinear Schrödinger equations with alternate signs of nonlinearities," *Europhysics letters*, vol. 127, no. 5, article 50005, 2019.

[2] W. Q. Peng, S. F. Tian, and T. T. Zhang, "Dynamics of breather waves and higher-order rogue waves in a coupled nonlinear Schrödinger equation," *Europhysics Letters*, vol. 123, no. 5, article 50005, 2018.

[3] J. Tamang, K. Sarkar, and A. Saha, "Solitary wave solution and dynamic transition of dust ion acoustic waves in a collisional nonextensive dusty plasma with ionization effect," *Physica A: Statistical Mechanics and its Applications*, vol. 505, pp. 18–34, 2018.

[4] A. Saha and S. Banerjee, "Comment on "multi-dimensional instability of dust acoustic waves in magnetized quantum plasmas with positive or negative dust"," *Brazilian Journal of Physics*, vol. 51, no. 4, pp. 1127-1128, 2021.

[5] J. Tamang and A. Saha, "Influence of dust-neutral collisional frequency and nonextensivity on dynamic motion of dust-acoustic waves," *Waves in Random and Complex Media*, vol. 31, no. 4, pp. 597–617, 2021.

[6] S. A. EI-Tantawy and A. M. Wazwaz, "Anatomy of modified Korteweg-de Vries equation for studying the modulated envelope structures in non-Maxwellian dusty plasmas: freak waves and dark soliton collisions," *Physics of Plasmas*, vol. 25, no. 9, article 092105, 2018.

[7] A. M. Wazwaz, "New solitons and kink solutions for the Gardner equation," *Communications in Nonlinear Science and Numerical Simulation*, vol. 12, no. 8, pp. 1395–1404, 2007.

[8] S. A. EI-Tantawy, "Nonlinear dynamics of soliton collisions in electronegative plasmas: the phase shifts of the planar KdV- and mkdV-soliton collisions," *Chaos, Solitons and Fractals*, vol. 93, pp. 162–168, 2016.

[9] S. A. EI-Tantawy and P. Carbonaro, "Nonplanar ion-acoustic solitons collision in $Xe^+ - F^- - SF_6^-$ and $Ar^+ - F^- - SF_6^-$ plasmas," *Physics Letters A*, vol. 380, no. 18-19, pp. 1627–1634, 2016.

[10] D. J. Kaup, "Variational solutions for the discrete nonlinear Schrodinger equation," *Mathematics and Computers in Simulation*, vol. 69, no. 3-4, pp. 322–333, 2005.

[11] M. Wadati, "Transformation theories for nonlinear discrete systems," *Progress of Theoretical Physics Supplement*, vol. 59, pp. 36–63, 1976.

[12] M. Toda, *Theory of Nonlinear Lattices*, Springer, Berlin, 1989.

[13] M. J. Ablowitz and P. A. Clarkson, *Solitons, Nonlinear Evolution Equations and Inverse Scattering*, Cambridge University Press, Cambridge, 1991.

[14] R. Hirota, "Exact N-soliton solution of a nonlinear lumped network equation," *Journal of the Physical Society of Japan*, vol. 35, no. 1, pp. 286–288, 1973.

[15] X. B. Hu and Y. T. Wu, "Application of the Hirota bilinear formalism to a new integrable differential- difference equation," *Physics Letters A*, vol. 246, no. 6, pp. 523–529, 1998.

[16] X. G. Geng, "Darboux transformation of the discrete Ablowitz-Ladik eigenvalue problem," *Acta Mathematica Scientia*, vol. 9, no. 1, pp. 21–26, 1989.

[17] X. X. Xu, "A deformed reduced semi-discrete Kaup-Newell equation, the related integrable family and Darboux transformation," *Applied Mathematics and Computation*, vol. 251, pp. 275–283, 2015.

[18] H. T. Wang and X. Y. Wen, "Soliton elastic interactions and dynamical analysis of a reduced integrable nonlinear Schrödinger system on a triangular-lattice ribbon," *Nonlinear Dynamics*, vol. 100, no. 2, pp. 1571–1587, 2020.

[19] T. Xu, H. J. Li, H. J. Zhang, M. Li, and S. Lan, "Darboux transformation and analytic solutions of the discrete PT-symmetric nonlocal nonlinear Schrödinger equation," *Applied Mathematics Letters*, vol. 63, pp. 88–94, 2017.

[20] F. J. Yu and S. Feng, "Explicit solution and Darboux transformation for a new discrete integrable soliton hierarchy with 4x4 Lax pairs," *Mathematical Methods in the Applied Sciences*, vol. 40, no. 15, pp. 5515–5525, 2017.

[21] Y. Yang and Y. Zhu, "Darboux-Backlund transformation, breather and rogue wave solutions for Ablowitz-Ladik equation," *Optik*, vol. 217, article 164920, 2020.

[22] Y. Zhu, Y. Yang, and X. Li, "Darboux-Backlund transformation, breather and rogue wave solutions for the discrete Hirota equation," *Optik*, vol. 236, article 166647, 2021.

[23] X. Y. Wen and Y. T. Gao, "Darboux transformation and explicit solutions for discretized modified Korteweg-de Vries lattice equation," *Communications in Theoretical Physics*, vol. 53, pp. 825–830, 2010.

[24] X. Y. Wen, Z. Y. Yan, and B. A. Malomed, "Higher-order vector discrete rogue-wave states in the coupled Ablowitz-Ladik equations: exact solutions and stability," *Chaos*, vol. 26, no. 12, article 123110, 2016.

[25] X. Y. Wen, Z. Y. Yan, and G. Q. Zhang, "Nonlinear self-dual network equations: modulation instability, interactions of higher order discrete vector rational solitons and dynamical behaviours," *Proceedings of The Royal Society A-Mathematical Physical And Engineering Sciences*, vol. 476, no. 2242, article 20200512, 2020.

[26] Y. B. Suris, *The Problem of Integrable Discretization: Hamiltonian Approach*, Birkhäuser Verlag, Basel, 2003.

[27] Z. Wang, L. Zhou, and H. Q. Zhang, "Solitary solution of discrete mKdV equation by homotopy analysis method," *Communications in Theoretical Physics*, vol. 49, pp. 1373–1378, 2008.

[28] K. Narita, "N-soliton solution of a lattice equation related to the discrete MKdV equation," *Journal of Mathematical Analysis And Applications*, vol. 381, no. 2, pp. 963–965, 2011.

[29] T. Zhou, Z. N. Zhu, and P. He, "A fifth order semidiscrete mKdV equation," *Science China-Mathematics*, vol. 56, no. 1, pp. 123–134, 2013.

[30] Z. Xiao, K. Li, and J. Zhu, "Multiple-pole solutions to a semi-discrete modified Korteweg-de Vries equation," *Advances in Mathematical Physics*, vol. 2019, Article ID 5468142, 8 pages, 2019.

[31] C. Koroglu and A. Aydin, "An unconventional finite difference scheme for modified Korteweg-de Vries equation," *Advances in Mathematical Physics*, vol. 2017, Article ID 4796070, 9 pages, 2017.

[32] J. F. Liang and X. Wang, "Investigation of interaction solutions for modified Korteweg-de Vries equation by consistent Riccati expansion method," *Mathematical Problems in Engineering*, vol. 2019, Article ID 9535294, 8 pages, 2019.

[33] M. Wadati, "The exact solution of the modified Korteweg-de Vries equation," *Journal of the Physical Society of Japan*, vol. 32, no. 6, pp. 1681–1687, 1972.

[34] M. Wadati, "The modified Korteweg-de Vries equation," *Journal of the Physical Society of Japan*, vol. 34, no. 5, pp. 1289–1296, 1973.

[35] R. Hirota, "Exact solution of theModifiedKorteweg-de Vries equation for multiple collisions of solitons," *Journal of the Physical Society of Japan*, vol. 33, no. 5, pp. 1456–1458, 1972.

[36] J. L. Ji and Z. N. Zhu, "On a nonlocal modified Korteweg-de Vries equation: integrability, Darboux transformation and soliton solutions," *Communications in Nonlinear Science and Numerical Simulation*, vol. 42, pp. 699–708, 2017.

[37] G. P. Agrawal, *Nonlinear Fiber Optics*, Academic Press, New York, 2001.

[38] E. F. El-Shamy, "Dust-ion-acoustic solitary waves in a hot magnetized dusty plasma with charge fluctuations," *Chaos, Solitons Fractals*, vol. 25, no. 3, pp. 665–674, 2005.

[39] Y. R. Shi, J. Zhang, H. J. Yang, and W. S. Duan, "Single soliton of double kinks of the mKdV equation and its stability," *Acta Physica Sinica*, vol. 59, no. 11, pp. 7564–7569, 2010.

[40] M. J. Ablowitz and J. F. Ladik, "On the solution of a class of nonlinear partial difference equations," *Studies in Applied Mathematics*, vol. 57, no. 1, pp. 1–12, 1977.

[41] M. J. Ablowitz and J. F. Ladik, "Nonlinear differential-difference equations," *Journal of Mathematical Physics*, vol. 16, no. 3, pp. 598–603, 1975.

[42] L. N. Trefethen, *Spectral Methods in MATLAB*, SIAM, Philadelphia, 2000.

[43] X. H. Meng, X. Y. Wen, L. H. Piao, and D. S. Wang, "Determinant solutions and asymptotic state analysis for an integrable model of transient stimulated Raman scattering," *Optik*, vol. 200, article 163348, 2020.

[44] C. Zhang and G. Chen, "The soliton solutions and long-time asymptotic analysis for a general coupled KdV equation," *Advances in Mathematical Physics*, vol. 2021, Article ID 5569909, 6 pages, 2021.

[45] C. L. Yuan, X. Y. Wen, H. T. Wang, and Y. Q. Liu, "Soliton interactions and their dynamics in a higher-order nonlinear self-dual network equation," *Chinese Journal of Physics*, vol. 64, pp. 45–53, 2020.